

Complexes of carbene analogs with Lewis bases: matrix IR spectroscopy and quantum-chemical studies*

S. E. Boganov, V. I. Faustov, M. P. Egorov,* and O. M. Nefedov

N. D. Zelinsky Institute of Organic Chemistry, Russian Academy of Sciences,
47 Leninsky Pros., 119991 Moscow, Russian Federation.
Fax: (095) 135 5328. E-mail: mpe@ioc.ac.ru

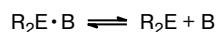
The results of studies on complexes of carbene analogs ER_2 ($E = Si, Ge, Sn, Pb$) with Lewis bases by matrix IR spectroscopy and quantum chemistry methods are considered. Trends in changes in the spectral characteristics, structures, and stability of the complexes are outlined.

Key words: carbene analogs, silylenes, germynes, stannylens, plumbylens, complexes with Lewis bases, matrix IR spectroscopy, quantum-chemical calculations.

Introduction

Donor-acceptor interactions responsible for the formation of complexes of different stability are typical of electron-deficient, coordinatively unsaturated molecules including carbenes and their analogs, namely, silylenes, germynes, stannylens, and plumbylens (see, e.g., reviews^{1–6} and references cited therein). These interactions also underlie numerous transformations of chemical compounds.

Carbene analogs (CAs) ER_2 ($E = Si, Ge, Sn, Pb$) are characterized by extremely high reactivities. They are the key intermediates of many reactions of organosilicon, organogermanium, and organotin compounds including industrially important reactions.^{7,8} The vast majority of experimentally studied CAs** have a singlet ground state, a nonbonding σ -orbital filled with two electrons, and a low-lying π -orbital. This allows these species to be involved in donor-acceptor interactions with Lewis acids and bases. These interactions are responsible for stabilization of divalent state of the central heteroatom in the CA molecules,^{3–5,11} for significant changes in the spectral properties of these species,^{4,12} and to a great extent for the reactivity and reaction mechanisms of CAs.^{4,5,13} In particular, kinetic studies revealed that complexes of CAs are much less reactive than free unbound CAs. It was also pointed out that in the case of dynamical equilibrium



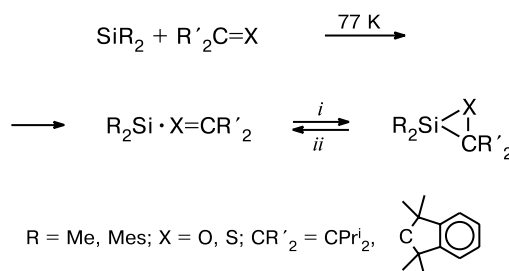
(B is a Lewis base) the reaction under study can proceed involving the unbound CA present in the reaction mix-

ture rather than its complex.¹⁴ Carbene analogs can form not only intermolecular but also intramolecular complexes owing to coordination of the carbene center to the heteroatoms present in the substituent R.^{11,15,16}

The binding energies of the complexes of CAs vary over a rather wide range from several tens of kcal mol^{–1} for stable complexes with transition metal compounds $L_nM=ER_2$ ($L_nM=ER_2 \cdot B$)¹⁷ or for stable complexes of dihalo-substituted CAs with relatively strong Lewis bases (ethers, phosphines, amines; see reviews^{3,11}) to a few kcal mol^{–1} for the complexes with weak Lewis bases (alkenes, alkynes, halogen-containing compounds).¹² Loosely bound, highly labile complexes formed as intermediates of numerous reactions of CAs are still poorly studied.

The authors of many studies^{3–6,12,13} suggested the formation of weak pre-reaction complexes in reactions of CAs with various substrates. This has been supported by the data of UV spectroscopic studies in glassy hydrocarbon matrices and in the liquid phase. For instance, labile complexes of silylenes and germynes with alcohols, ethers, thioethers, ketones, thioetones, amines, phosphines, and organochlorine compounds^{4,12} and a com-

Scheme 1



Conditions: glassy hydrocarbon matrix; *i.* 460 nm or annealing; *ii.* 254 nm.

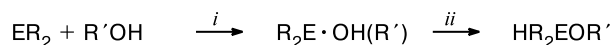
* Based on the materials presented at the VII International Conference "Chemistry of Carbenes and Related Intermediates" (Kazan, Russia, June 23–26, 2003).

** The exceptions are the sterically hindered silylene $Si(SiBu^t_3)_2$ ⁹ and, probably, $Si(SiBu^t_3)SiPr^i_3$ and $Si(SiPr^i_3)_2$.¹⁰

plex $((\text{Me}_3\text{Si})_2\text{CH})_2\text{Sn} \cdot \text{S}=\text{C}=\text{C}\text{Bu}^t_2$ **18** were detected using UV spectroscopy in glassy hydrocarbon matrices and laser flash photolysis in organic solvents. Annealing of matrices containing complexes of silylenes SiR_2 ($\text{R} = \text{Me}, \text{Mes}$; $\text{Mes} = 2,4,6\text{-trimethylphenyl}$)¹⁹ with ketones and thioketones led to reversible addition of silylene to the double bonds $\text{C}=\text{O}$ and $\text{C}=\text{S}$ (Scheme 1).

Analogously, annealing of glassy hydrocarbon matrices containing complexes of labile silylenes²⁰ and germynes²¹ with alcohols resulted in corresponding alkoxy silanes and alkoxygermanes (Scheme 2).

Scheme 2



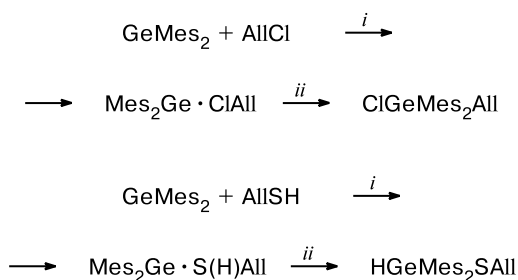
$\text{ER}_2 = \text{SiMe}_2, \text{SiMes}_2, \text{SiBu}^t\text{Mes}, \text{Si}(\text{OC}_6\text{H}_3\text{Pr}^i_2\text{-}2,6)\text{Mes}$;
 $\text{R}' = \text{Pr}^i, \text{Bu}^s$;

$\text{ER}_2 = \text{GePh}_2, \text{GeMes}_2, \text{Ge}(2,6\text{-Et}_2\text{C}_6\text{H}_3)_2$; $\text{R}' = \text{Et}, \text{Pr}^i, \text{Bu}^s, \text{Bu}^t$

Conditions: 3-methylpentane—*isopentane* (3 : 7); *i.* 77 K;
ii. annealing matrix.

Annealing of matrices containing complexes of GeMe_2 with allyl chloride or allyl mercaptane gave products of germylene insertion into the $\text{C}-\text{Cl}$ and $\text{S}-\text{H}$ bonds, respectively (Scheme 3).^{21,22}

Scheme 3



Conditions: 3-methylpentane—*isopentane* (3 : 7); *i.* 77 K;
ii. annealing.

Experimentally, short-lived CAs are successfully detected by laser flash photolysis. Using this technique, complexes of GeMe_2 with PPh_3 ^{23–26} and of SiMe_2 with CHBr_3 ²⁷ and CCl_4 ²⁸ were detected in the liquid phase. The last-named two complexes were formed during the SiMe_2 insertion into the corresponding $\text{C}-\text{Hal}$ bonds.

Matrix IR spectroscopy^{29–31} belongs to the most efficient methods of investigations of intermediates of chemical reactions. This technique involves stabilization of an intermediate under study in a rigid noble-gas matrix at helium temperatures (4–20 K) and analysis of its IR spectrum. Of considerable importance for the interpretation

of experimental data and detalization of the general pattern of the interactions under study are the results of quantum-chemical calculations. In this review we consider the available results of (i) matrix IR spectroscopy studies on complexation of CAs and (ii) quantum-chemical studies of the experimentally investigated systems.

Complexes of carbene analogs with N_2 , NO , CO , H_2 , and O_2

The electronic structure of dinitrogen molecule allows this species to be considered as a weak Lewis base. This was confirmed in a series of studies on complexation of N_2 with various Lewis acids.^{32,33} Though dinitrogen is a very weak base, its complexes with many dihalo-substituted CAs (SiCl_2 ,³⁴ SnF_2 ,³⁵ SnCl_2 , PbF_2 ³⁶) were successfully detected by matrix IR spectroscopy.

A general experimental method of investigation of these complexes and the complexes described below was as follows. A molecular beam of CAs generated by evaporation of corresponding dihalides EHal_2 ^{35,36} or by pyrolysis of appropriate precursor (in the case of SiCl_2 , decomposition of Si_2Cl_6 at 850 °C was employed³⁴) was co-deposited with a large excess of the matrix gas (Ar) containing a small specified amount of N_2 on a support placed in an evacuated cryostat and cooled down to helium temperatures. The formation of matrix was followed by recording its IR spectrum. New spectral bands were assigned to corresponding complexes based on the following grounds. The intensities of the new bands changed simultaneously on change in the relative concentrations of the reactant molecules, while the positions of band maxima remained unchanged as the CAs : N_2 : Ar mole ratio varied over a wide range. This pointed to the fact that the new bands are characteristic of the same stable (under the matrix conditions) compounds of constant composition, which were formed in the reactions of CAs with N_2 . When CAs were generated by pyrolysis of precursor, the possibility of interaction of the precursor and other (non-CA) products of its decomposition with N_2 was additionally studied. For instance, studies on the reaction of SiCl_2 revealed that neither its precursor, Si_2Cl_6 , nor SiCl_4 (the only stable product of thermal decomposition of Si_2Cl_6) can form products of interaction with N_2 in Ar matrices. The new bands were observed near the bands of CAs, thus indicating minor changes in the molecular geometries and force fields upon the formation of reaction product and, hence, a weak interaction. Based on statistical grounds, the detection of these bands at rather low concentrations of both CAs and N_2 (usually, at most 0.5%) pointed that at most one molecule of each reactant was involved in complexation. Controlled annealing of matrices (in the 35–45 K interval for Ar matrices; in this temperature range, the matrix becomes less

Table 1. Vibrational frequencies (ν_i/cm^{-1}) of the complexes of CAs with N_2 in low-temperature argon matrices and their absolute^a ($\Delta\nu_i$) and relative^b ($\Delta\nu_i^{\text{rel}}$) shifts with respect to the corresponding frequencies of the starting reagents

Complex	ν_i	$\Delta\nu_i/\text{cm}^{-1}$	$\Delta\nu_i^{\text{rel}} (\%)$	Reference
$\text{Cl}_2\text{Si} \cdot \text{N}_2$	511.2 $\nu^s(\text{Si}-\text{Cl}, {}^{28}\text{Si}^{35}\text{Cl}_2)$	1.0	0.2	34
	508.9 $\nu^s(\text{Si}-\text{Cl}, {}^{28}\text{Si}^{35}\text{Cl}^{37}\text{Cl})$	0.9	0.2	34
	506.5 $\nu^s(\text{Si}-\text{Cl}, {}^{29}\text{Si}^{35}\text{Cl}_2)$	0.7	0.1	34
	500.1 $\nu^{\text{as}}(\text{Si}-\text{Cl}, {}^{28}\text{Si}^{35}\text{Cl}_2)$	1.2	0.2	34
	496.9 $\nu^{\text{as}}(\text{Si}-\text{Cl}, {}^{28}\text{Si}^{35}\text{Cl}^{37}\text{Cl})$	0.9	0.2	34
	495.1 $\nu^{\text{as}}(\text{Si}-\text{Cl}, {}^{28}\text{Si}^{37}\text{Cl}_2 \text{ and } {}^{29}\text{Si}^{35}\text{Cl}_2)$	0.8	0.2	34
$\text{F}_2\text{Sn} \cdot \text{N}_2$	588 $\nu^s(\text{Sn}-\text{F})$	5	0.8	35
	565 $\nu^{\text{as}}(\text{Sn}-\text{F})$	6	1.1	35
$\text{Cl}_2\text{Sn} \cdot \text{N}_2$	329.8 $\nu^{\text{as}}(\text{Sn}-\text{Cl}, \text{Sn}^{35}\text{Cl}_2)$	4.4	1.3	36
	326.7 $\nu^{\text{as}}(\text{Sn}-\text{Cl}, \text{Sn}^{35}\text{Cl}^{37}\text{Cl})$	3.2	1.0	36
$\text{F}_2\text{Pb} \cdot \text{N}_2$	526.6 $\nu^s(\text{Pb}-\text{F})$	4.8	0.9	36
	502.2 $\nu^{\text{as}}(\text{Pb}-\text{F})$	5.0	1.0	36
$\text{Cl}_2\text{Si} \cdot 2\text{N}_2$	498.7 $\nu^{\text{as}}(\text{Si}-\text{Cl}, {}^{28}\text{Si}^{35}\text{Cl}_2)$	2.6	0.5	34
	493.5 $\nu^{\text{as}}(\text{Si}-\text{Cl}, {}^{28}\text{Si}^{37}\text{Cl}_2 \text{ and } {}^{29}\text{Si}^{35}\text{Cl}_2)$	2.4	0.5	34
$\text{F}_2\text{Sn} \cdot 2\text{N}_2$	583 $\nu^s(\text{Sn}-\text{F})$	10	1.7	35
	557 $\nu^{\text{as}}(\text{Sn}-\text{F})$	14	2.5	35
$\text{Cl}_2\text{Sn} \cdot 2\text{N}_2$	326.1 $\nu^{\text{as}}(\text{Sn}-\text{Cl}, \text{Sn}^{35}\text{Cl}_2)$	8.1	2.4	36
	322.3 $\nu^{\text{as}}(\text{Sn}-\text{Cl}, \text{Sn}^{35}\text{Cl}^{37}\text{Cl})$	7.6	2.3	36
$\text{Cl}_2\text{Si} \cdot x\text{N}_2, x > 2^c$	509.6 $\nu^s(\text{Si}-\text{Cl}, {}^{28}\text{Si}^{35}\text{Cl}_2)$	2.6	0.5	34
	$\nu^s(\text{Si}-\text{Cl}, \text{other isotopomers})$	2.1–2.4	0.4	34
	496.4 $\nu^{\text{as}}(\text{Si}-\text{Cl}, {}^{28}\text{Si}^{35}\text{Cl}_2)$	4.9	1.0	34
	$\nu^{\text{as}}(\text{Si}-\text{Cl}, \text{other isotopomers})$	4.2–4.9	0.8	34
$\text{Cl}_2\text{Sn} \cdot x\text{N}_2, x > 2^c$	318 $\nu^{\text{as}}(\text{Sn}-\text{Cl}, \text{Sn}^{35}\text{Cl}_2)$	36	11	36
	316 $\nu^{\text{as}}(\text{Sn}-\text{Cl}, \text{Sn}^{35}\text{Cl}^{37}\text{Cl})$	36	11	36

^a $\Delta\nu_i = \nu_i^{\text{free}} - \nu_i^{\text{compl}}$ (ν_i^{free} are the frequencies of the starting reagent).^b $\Delta\nu_i^{\text{rel}} = |\Delta\nu_i/\nu_i^{\text{free}}| \cdot 100$.^c In N_2 matrix.

rigid and isolated molecules interact with one another by diffusion) resulted in an increase in the band intensities of complexes due to the formation of extra amounts of complexes and in some cases in the appearance of bands of $\text{CAs} \cdot 2\text{N}_2$ complexes (the 1 : 2 complexes) followed by weakening and disappearance of these bands owing to oligomerization of CAs. The bands of complexes disappeared only after disappearance of the bands of unbound CA; *i.e.*, complexes were less prone to oligomerization compared to monomeric CAs. In some cases, the 1 : 2 complexes were detected immediately after matrix formation at higher concentrations of N_2 . A considerable increase in the concentration of CA in the matrix, which is necessary for the formation of 2 : 1 complexes, led to oligomerization of CAs; because of this, such complexes were not detected. Table 1 lists the vibrational frequencies of complexes of CAs with N_2 in Ar matrices.

The structure and stability of experimentally detected complexes were studied by various quantum chemistry methods. These are MP2/3-21G(d)//HF/3-21G(d) for $\text{F}_2\text{Sn} \cdot \text{N}_2$ and $\text{F}_2\text{Sn} \cdot 2\text{N}_2$,³⁵ PBE/TZ2P, B3LYP/6-311+G(d), and G2(MP2,SVP) for $\text{Cl}_2\text{Si} \cdot \text{N}_2$,³⁴ and PBE/TZ2P for $\text{Cl}_2\text{Si} \cdot 2\text{N}_2$, $\text{Cl}_2\text{E} \cdot \text{N}_2$ and $\text{Cl}_2\text{E} \cdot 2\text{N}_2$

(E = Ge, Sn).³⁴ In all cases, the energy minima corresponding to molecular complexes were located on the PES of the systems $\text{EHal}_2 + \text{N}_2$. The axis of the N_2 molecule in complexes is directed nearly normal to the CA plane (Fig. 1). The bonding occurs due to the interaction between the lone electron pair (LEP) of one N atom and the vacant p-orbital localized on the central atom of CA. No minima corresponding to other orientations of N_2 molecules relative to CA (*e.g.*, π -complexes) were located on the PES of these systems.

The calculated geometric parameters of complexes and those of the starting CA and N_2 molecules are listed in Table 2. They are in good agreement with the available experimental values for CAs and N_2 . From the data listed in Table 2 it follows that the geometry of the reagents

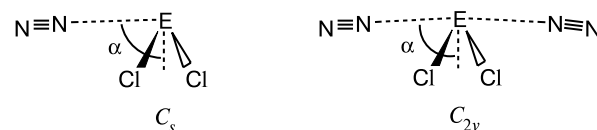
**Fig. 1.** Calculated structures of complexes of carbene analogs ECl_2 (E = Si, Ge, Sn) with N_2 . Given are the symmetry groups.

Table 2. Calculated and experimental complexation energies ($\Delta E_{\text{form}}/\text{kcal mol}^{-1}$), geometric parameters (interatomic distances (d) and angles), and dipole moments (μ) of the starting molecules (CAs and N_2) and their complexes

Compound	Method ^a	$-\Delta E_{\text{form}}^b$	$d/\text{\AA}$			Angle/deg			μ/D	Reference
			E—Hal	N—N	E—N	α^c	Hal—E—Hal	N≡N—E		
N_2	PBE	—	—	1.103	—	—	—	—	0	34
	B3LYP	—	—	1.096	—	—	—	—	0	34
	HF	—	—	1.073	—	—	—	—	0	35
	Experiment	—	—	1.098	—	—	—	—	—	37
SiCl_2	PBE	—	2.116	—	—	—	101.8	—	1.1	34
	B3LYP	—	2.109	—	—	—	102.1	—	1.5	34
	Experiment	—	2.065310	—	—	—	101.324	—	—	38
$\text{Cl}_2\text{Si} \cdot \text{N}_2$	PBE	0.3	2.119	1.103	3.489	87	101.6	173	1.2	34
	B3LYP	0.3 ^d	2.111	1.095	3.540	—	102.0	—	1.6	34
	G2	1.2	—	—	—	—	—	—	—	34
$\text{Cl}_2\text{Si} \cdot 2\text{N}_2$	PBE	0.6	2.230	1.103	3.525	87	101.5	171	1.2	34
GeCl_2	PBE	—	2.221	—	—	—	100.9	—	2.1	34
	Experiment	—	2.169452	—	—	—	99.882	—	—	39
$\text{Cl}_2\text{Ge} \cdot \text{N}_2$	PBE	0.7	2.225	1.103	3.311	87	100.8	170	2.2	34
$\text{Cl}_2\text{Ge} \cdot 2\text{N}_2$	PBE	1.0	2.229	1.103	3.327	84	100.7	166	2.3	34
SnF_2	MP2//HF	—	1.870	—	—	—	94	—	2.4	35
	Experiment	—	1.893	—	—	—	96	—	—	40
$\text{F}_2\text{Sn} \cdot \text{N}_2$	MP2//HF	4.6 ^e	1.875	1.074	2.900	76	94	167	2.3	35
$\text{F}_2\text{Sn} \cdot 2\text{N}_2$	MP2//HF	8.9 ^e	1.879	1.074	2.937	63	94	166	1.6	35
SnCl_2	PBE	—	2.409	—	—	—	98.8	—	3.0	34
	Experiment	—	2.335	—	—	—	99.1	—	—	41
$\text{Cl}_2\text{Sn} \cdot \text{N}_2$	PBE	0.9	2.415	1.102	3.313	80	98.7	168	3.1	34
$\text{Cl}_2\text{Sn} \cdot 2\text{N}_2$	PBE	1.5	2.420	1.102	3.326	77	98.6	165	3.0	34

^a The computational methods are denoted as follows: PBE is PBE/TZ2P, B3LYP is B3LYP/6-311+G(d), G2 is G2(MP2,SVP), and MP2//HF is MP2/3-21G(d)//HF/3-21G(d).

^b Calculated for 0 K with inclusion of zero-point vibrational energy correction.

^c The angle α is shown in Fig. 1.

^d $\Delta G = 4.3 \text{ kcal mol}^{-1}$; calculated for $p = 1 \text{ atm}$ and $T = 298 \text{ K}$ with inclusion of zero-point vibrational energy correction.

^e With inclusion of the basis set superposition error.

remains virtually unchanged upon complexation, which causes only a slight elongation of the E—Hal bond (the magnitude of the elongation for the 1 : 2 complexes is twice as large as for the 1 : 1 complexes). The E...N distances in the complexes are rather long ($\sim 3.5 \text{ \AA}$), being even longer in the complexes with two N_2 molecules. The complexation energies are rather low, from a few tenths of a kcal mol^{-1} to several kcal mol^{-1} (see Table 2). It should be noted that the G2(MP2,SVP) calculated estimate of the binding energy of the complex $\text{Cl}_2\text{Si} \cdot \text{N}_2$ ($1.2 \text{ kcal mol}^{-1}$) is higher than those obtained from PBE/TZ2P and B3LYP/6-311+G(d) calculations ($0.3 \text{ kcal mol}^{-1}$). High accuracy of the G2(MP2,SVP) method suggests that methods based on density functional theory (DFT) somewhat underestimate the complexation energy. The formation of 1 : 2 complexes is

nearly two times more energetically favorable than the formation of 1 : 1 complexes (see Table 2); *i.e.*, coordination of one N_2 molecule has virtually no effect on complexation with the second N_2 molecule. This means that the reactivities of EHal_2 species must not be significantly influenced by the complexation with N_2 . Usually, complexation causes a slight change in the dipole moment (see Table 2), thus indicating a low degree of electron density transfer in the complexes.

Density functional calculations underestimate the E—Cl stretching vibration frequencies of both the starting ECl_2 molecules and their complexes by $\sim 20 \text{ cm}^{-1}$ (Table 3), whereas the HF/3-21G(d) calculated frequencies of SnF_2 and its complexes are considerably overestimated. At the same time all computational methods satisfactorily (DFT methods — quite correctly) reproduce the

Table 3. Selected calculated and experimental^a vibrational frequencies (δ and ν/cm^{-1}) and band intensities^b ($I/\text{km mol}^{-1}$) in the IR spectra of the starting CAs and N_2 and their complexes

Compound	Method ^c	$\nu(\text{N}\equiv\text{N})$ (I)	$\nu^s(\text{E}-\text{Hal})$ (I)	$\Delta\nu^s(\text{E}-\text{Hal})^d$	$\nu^{\text{as}}(\text{E}-\text{Hal})$ (I)	$\Delta\nu^{\text{as}}(\text{E}-\text{Hal})^d$	$\delta(\text{HalEHal})$ (I)	Reference
N_2	PBE	2330.8 (0.0)	—	—	—	—	—	
	B3LYP	2444.9 (0.0)	—	—	—	—	—	
SiCl_2	PBE	—	490.0 (71)	—	482.7 (182)	—	182.5 (1.0)	34
	B3LYP	—	489.0 (95)	—	477.4 (217)	—	194.4 (2.3)	34
	Experiment	—	521.6 ^e	—	502 ^e	—	200.6 ^e	12
$\text{Cl}_2\text{Si}\cdot\text{N}_2$	PBE	2344.1 (0.2)	487.2 (69)	2.8	478.4 (178)	4.3	184.0 (1.1)	34
	B3LYP	2447.0 (0.3)	487.4 (92)	1.6	474.3 (211)	3.1	193.6 (1.9)	34
$\text{Cl}_2\text{Si}\cdot 2\text{N}_2$	PBE	2342.5 (0.1), 2342.4 (0.1)	487.1 (67)	2.9	476.5 (174)	6.2	182.1 (0.8)	34
GeCl_2	PBE	—	380.4 (43)	—	361.1 (114)	—	143.2 (1.6)	34
	Experiment	—	391 ^e	—	372 ^e	—	159 ^e	12
$\text{Cl}_2\text{Ge}\cdot\text{N}_2$	PBE	2345.4 (0.6)	378.2 (42)	2.2	357.3 (111)	3.8	144.2 (1.5)	34
$\text{Cl}_2\text{Ge}\cdot 2\text{N}_2$	PBE	2343.8 (0.4), 2345.2 (0.5)	375.4 (41)	5.0	353.7 (109)	7.4	144.9 (0.9)	34
SnF_2	HF	—	749	—	730	—	251	35
	Experiment	—	592.7 ^f	—	570.9 ^f	—	180 ^e	12
$\text{F}_2\text{Sn}\cdot\text{N}_2$	HF	2757	742	7	723	7	253	35
$\text{F}_2\text{Sn}\cdot 2\text{N}_2$	HF	2756, 2756	736	13	717	13	254	35
SnCl_2	PBE	—	338.8 (42)	—	325.5 (88)	—	113.3 (2.6)	34
	Experiment	—	350 ^e	—	344 ^e	—	120 ^e	12
$\text{Cl}_2\text{Sn}\cdot\text{N}_2$	PBE	2346.6 (1.0)	336.1 (42)	2.7	321.1 (87)	4.4	111.7 (2.1)	34
$\text{Cl}_2\text{Sn}\cdot 2\text{N}_2$	PBE	2346.1 (0.8), 2344.6 (0.8)	333.4 (41)	5.4	318.4 (85)	7.1	107.2 (0.9)	34

^a Experimental frequencies of the complexes are listed in Table 1.^b Listed are the data for the most abundant isotopes of the molecule-constituting elements.^c The computational methods are denoted as follows: PBE is PBE/TZ2P, B3LYP is B3LYP/6-311+G(d), and HF is HF/3-21G(d).^d $\Delta\nu_i = \nu_i(\text{CA}) - \nu_i^{\text{compl}}$ ($\nu_i(\text{CA})$ is the frequency of unbound CA).^e In the gas phase.^f In Ar matrix.

frequency shifts upon complexation (see Table 3). Calculations predict a decrease in the E—Hal stretching vibration frequencies upon complexation, the frequency shift of the symmetric stretching vibration (ν^s) being slightly smaller than that of the antisymmetric vibration (ν^{as}), which is consistent with experimental data. Noteworthy is that the intensities of the stretching vibration bands remain almost unchanged upon complexation (see Table 3). This permits estimation of the relative amount of CAs and their complexes in matrices by comparing the corresponding band intensities. B3LYP calculations excellently reproduce the experimentally observed isotopic structure of spectral bands for both SiCl_2 and $\text{Cl}_2\text{Si}\cdot\text{N}_2$.³⁴ According to calculations, the frequency differences between the isotopic band components remain unchanged upon complexation with N_2 molecule; this fact was used³⁴ in assigning the bands of different isotopomers of the complexes of SiCl_2 . Complexation causes some polarization of the

$\text{N}\equiv\text{N}$ bond. Because of this, the $\text{N}\equiv\text{N}$ stretching vibration intensity differs from zero, being at the same time nearly three orders of magnitude lower than the intensities of E—Hal stretching vibrations. That is why the $\text{N}\equiv\text{N}$ band was not detected experimentally for all complexes. At the same time the $\text{N}\equiv\text{N}$ stretching vibration band was recorded in the IR spectra of a complex of N_2 with SiCp^*_2 in cryosolutions at 2046 cm^{-1} in liquid Xe and at 2053 cm^{-1} in liquid N_2 owing to the use of cells with large optical path length.⁴²

Earlier,^{36,43} it was assumed that the relative frequency shifts of the E—Hal stretching vibrations upon complexation can serve as a measure of the strength of complexes. In the case of dichloro-substituted CAs this was substantiated by the results of quantum-chemical calculations.³⁴ Complexation of EHal_2 ($\text{E} = \text{Sn}, \text{Pb}$) with one and two N_2 molecules leads to a decrease in the E—Hal stretching vibration frequencies by ~ 1 and $\sim 2\%$, respectively (see

Table 1). The Si—Cl stretching vibration frequencies of the complexes $\text{Cl}_2\text{Si} \cdot \text{N}_2$ and $\text{Cl}_2\text{Si} \cdot 2\text{N}_2$ decrease only by 0.2 and 0.5%, respectively, thus pointing to a large decrease in the strength of complexes with N_2 on going from dihaloplumbylenes to dihalosilylenes. This conclusion was substantiated by the PBE/TZ2P calculated complexation energies of dichloro-substituted CAs with N_2 .³⁴ According to calculations,³⁴ the E—N distances (E = Ge, Sn) in both 1 : 1 and 1 : 2 complexes are nearly equal (see Table 2), being by about 0.2 Å shorter than in the corresponding complexes of SiCl_2 despite the smaller covalent radius of Si atom. This also indicates a much weaker interaction of SiCl_2 with N_2 .

In this connection it is noteworthy that dihalostannylenes and dihaloplumbylenes were completely bound into corresponding 1 : 1 complexes at 3–4 mol.% of N_2 in the matrix and that the formation of rather large amounts of 1 : 2 complexes was observed at the same concentrations.^{35,36} In the case of SiCl_2 the bands of free dichlorosilylene were observed even at N_2 concentration of 13 mol.%, the band intensities being comparable with those of the complex $\text{Cl}_2\text{Si} \cdot \text{N}_2$. On the contrary, the intensities of the bands assigned to the complex $\text{Cl}_2\text{Si} \cdot 2\text{N}_2$ remained low even at this, high concentration of dinitrogen. This means that in the case of SiCl_2 a much lower number of collisions between the CAs and N_2 molecules during the formation of the matrix causes the formation of complexes due to the much lower energy gains upon complexation of SiCl_2 with dinitrogen compared to the complexes of other EHal_2 (E = Sn, Pb) species.^{34,36}

The ability of CAs to form complexes with Lewis bases has been previously discussed in quantum-chemical studies on complexation of EH_2 (E = Si, Ge, Sn) with hydrides of Group 15 and 16 elements of the periodic system.⁴⁴ It was found that the acidity of EH_2 species reduces on going from silylene to stannylene. The effect of substituents in CAs on their acidities was not considered.⁴⁴ The

observed inversion of the acidity series of EHal_2 toward dinitrogen can be explained by the effects of both the nature of substituent at the carbene center and by the nature of the base. Indeed, most of the calculated complexation energies of EH_2 with rather strong bases exceeded 10 kcal mol⁻¹.⁴⁴ Though for the same base the complexation energies decreased on going from SiH_2 to SnH_2 , the magnitude of the decrease was strongly affected by the nature of the base and varied over a rather wide range. This seems to be associated with the specific features of the interaction in each particular case. Apparently, for weaker bases specific features of the interaction must play even more important role. Therefore, the acidity series⁴⁴ toward weak Lewis bases can be significantly changed even for EH_2 (E = Si, Ge, Sn).

Obviously, EHal_2 molecules react with dinitrogen to give some complexes only. In the case of SnF_2 , the results of quantum-chemical calculations confirmed that cycloaddition to the triple bond $\text{N} \equiv \text{N}$ is energetically unfavorable.³⁵

A possible implication is the conclusion that dinitrogen is undesired for using as the matrix gas in the matrix isolation studies of CAs. The vibrational spectra of SiCl_2 and SiBr_2 ,⁴⁵ GeF_2 ,⁴⁶ GeCl_2 , SnCl_2 , SnBr_2 , SnBrCl , PbBr_2 and PbBrCl ,⁴⁷ PbCl_2 ,^{47,48} and SiClMe , SiHMe and SiMe_2 ^{49,50} in N_2 matrices reported in the earlier studies seem to be the spectra of corresponding complexes with dinitrogen or of complex associates with more than two N_2 molecules. In the case of SiCl_2 ³⁴ and SnCl_2 ,³⁶ such associates detected in N_2 matrices were characterized by even lower E—Hal stretching vibration frequencies (see Table 1) compared to the complexes with two dinitrogen molecules (though this decrease could be due to the use of another matrix gas^{29,31} rather than the change in the composition of the complex). Noteworthy is that positions of the bands of SnF_2 isolated in N_2 matrix match those of the bands of the $\text{F}_2\text{Sn} \cdot 2\text{N}_2$ complex in Ar matrix.³⁵ By

Table 4. Infrared vibrational frequencies (ν_i) of complexes of CAs with NO, CO, O_2 , and H_2 in low-temperature argon matrices and their absolute^a ($\Delta\nu_i$) and relative^b ($\Delta\nu_i^{\text{rel}}$) shifts with respect to the corresponding frequencies of the starting reagents

Complex	ν_i	$\Delta\nu_i$	$\Delta\nu_i^{\text{rel}}$	Reference
	cm ⁻¹		(%)	
$\text{Cl}_2\text{Sn} \cdot \text{NO}$	1891.7 $\nu(\text{N—O})$	−16.7	0.9	36
	326.9 $\nu^{\text{as}}(\text{Sn—Cl}, \text{Sn}^{35}\text{Cl}_2)$	7.3	2.2	36
	323 $\nu^{\text{as}}(\text{Sn—Cl}, \text{Sn}^{35}\text{Cl}^{37}\text{Cl})$	7	2.1	36
$\text{F}_2\text{Pb} \cdot \text{NO}$	1891.4 $\nu(\text{N—O})$	−16.4	0.9	36
	522.6 $\nu^{\text{s}}(\text{Pb—F})$	8.8	1.7	36
	498.7 $\nu^{\text{as}}(\text{Pb—F})$	8.5	1.7	36
$\text{Cl}_2\text{Sn} \cdot \text{CO}$	2175.5 $\nu(\text{C—O})$	−37.5	1.8	36
	324.3 $\nu^{\text{as}}(\text{Sn—Cl}, \text{Sn}^{35}\text{Cl}_2)$	9.9	3.0	36
	319.9 $\nu^{\text{as}}(\text{Sn—Cl}, \text{Sn}^{35}\text{Cl}^{37}\text{Cl})$	10.0	3.0	36

(to be continued)

Table 4 (*continued*)

Complex	ν_i	$\Delta\nu_i$	$\Delta\nu_i^{\text{rel}}$	Reference
	cm ⁻¹		(%)	
$\text{Cl}_2\text{Sn} \cdot ^{13}\text{CO}$	2127.8 $\nu(^{13}\text{C}-\text{O})$	-36.4	1.7	36
	324.3 $\nu^{\text{as}}(\text{Sn}-\text{Cl}, \text{Sn}^{35}\text{Cl}_2)$	9.9	3.0	36
	319.9 $\nu^{\text{as}}(\text{Sn}-\text{Cl}, \text{Sn}^{35}\text{Cl}^{37}\text{Cl})$	10.0	3.0	36
$\text{F}_2\text{Pb} \cdot \text{CO}$	2176.4 $\nu(\text{C}-\text{O})$	-38.4	1.8	36
	520.6 $\nu^{\text{s}}(\text{Pb}-\text{F})$	10.8	2.0	36
	496.3 $\nu^{\text{as}}(\text{Pb}-\text{F})$	10.9	2.1	36
$\text{Cl}_2\text{Pb} \cdot \text{CO}$	2174.5 $\nu(\text{C}-\text{O})$	-36.5	1.7	36
	315.2 $\nu^{\text{s}}(\text{Pb}-\text{Cl})$	6.4	2.0	36
	292.6 $\nu^{\text{as}}(\text{Pb}-\text{Cl})$	7.3	2.4	36
$\text{Cl}_2\text{Pb} \cdot ^{13}\text{CO}$	2126 $\nu(\text{C}-\text{O})$	-34.6	1.7	36
	315.2 $\nu^{\text{s}}(\text{Pb}-\text{Cl})$	6.4	2.0	36
	292.6 $\nu^{\text{as}}(\text{Pb}-\text{Cl})$	7.3	2.4	36
$\text{Br}_2\text{Pb} \cdot \text{CO}$	2161.2 $\nu(\text{C}-\text{O})$	-23.2	1.1	36
$\text{I}_2\text{Pb} \cdot \text{CO}$	2162 or 2149 $\nu(\text{C}-\text{O})$	-24 or -11	1.1 or 0.5	36
$\text{H}_2\text{Si} \cdot \text{CO}$	2049.5, 2046.8, 2037.9 ^{c,d}	$\sim 100 \nu(\text{C}-\text{O})$	5	51
	$\nu(\text{C}-\text{O}), \nu^{\text{s}}(\text{Si}-\text{H})$ and $\nu^{\text{as}}(\text{Si}-\text{H})$	$\sim 75 \nu(\text{Si}-\text{H})$	4	51
	925.1 ^d $\delta(\text{CH}_2)$	70	7.0	51
	2054 and 2051 ^{e,f}			51
	$\nu(\text{C}-\text{O}), \nu^{\text{s}}(\text{Si}-\text{H})$ and $\nu^{\text{as}}(\text{Si}-\text{H})$			51
$\text{H}_2\text{Si} \cdot ^{13}\text{CO}$	912.5 ^e $\delta(\text{CH}_2)$			51
	2044.9 ^g $\nu^{\text{s}}(\text{Si}-\text{H})$ and $\nu^{\text{as}}(\text{Si}-\text{H})$	-86	4.4	51
	1996.0 $\nu(^{13}\text{C}-\text{O})$	95	4.5	51
$\text{D}_2\text{Si} \cdot \text{CO}$	918.5 $\delta(\text{CH}_2)$	77.5	7.8	51
	1490.9 $\nu^{\text{as}}(\text{Si}-\text{D})$	-61.8	4.3	51
	1479.1 $\nu^{\text{s}}(\text{Si}-\text{D})$	-52.2	3.7	51
$\text{Me}_2\text{Si} \cdot \text{CO}$	2043.9 $\nu(\text{C}-\text{O})$	94.1	4.4	51
	689.0 $\delta(\text{CD}_2)$	30.8	4.3	51
	1962 $\nu(\text{C}-\text{O})$	176	8.2	52
$\text{Me}_2\text{Si} \cdot ^{13}\text{CO}$	765 $\rho(\text{CH}_3)$	41	5.1	52
	1918 $\nu(^{13}\text{C}-\text{O})$	173	8.3	52
$\text{Me}_2\text{Si} \cdot \text{C}^{18}\text{O}$	765 $\rho(\text{CH}_3)$	41	5.1	52
	1915 $\nu(\text{C}-^{18}\text{O})$			52
$\text{O}=\text{C}=\text{Si} \cdot \text{H}_2$	765 $\rho(\text{CH}_3)$	41	5.1	52
$\text{O}=\text{C}=\text{Si} \cdot \text{H}_2$	1908 $\nu(\text{C}-\text{O})$	-8.1	0.4	51
	1745.3 $\nu(\text{C}\equiv\text{C})$	-4.3	0.2	54
$\text{HN}=\text{Si} \cdot \text{H}_2$	826.4 $\nu^{\text{s}}(\text{Si}-\text{C})$	0	0.0	54
	4178 $\nu(\text{H}-\text{H})$			55
$\text{DN}=\text{Si} \cdot \text{D}_2$	3580 $\nu(\text{N}-\text{H})$	5	0.1	55
	1200 $\nu(\text{Si}-\text{N})$	2	0.2	55
	522 $\delta(\text{N}-\text{H})$	0	0.0	55
$\text{F}_2\text{Si} \cdot \text{O}_2$	2994 $\nu(\text{D}-\text{D})$			55
$\text{F}_2\text{Si} \cdot \text{O}_2$	856.2 $\nu^{\text{as}}(\text{Si}-\text{F})$	-3.8	0.4	56
	847.3 $\nu^{\text{s}}(\text{Si}-\text{F})$	-4.8	0.6	56

^a $\Delta\nu_i = \nu_i^{\text{free}} - \nu_i^{\text{compl}}$ (ν_i^{free} are the frequencies of the starting reagent).

^b $\Delta\nu_i^{\text{rel}} = |\Delta\nu_i/\nu_i^{\text{free}}| \cdot 100$.

^c These three frequencies correspond to three normal vibrational modes listed below. Unambiguous assignment of each frequency to a particular normal vibration is impossible.

^d These bands were observed in the experimental studies of the interaction $\text{Si} + \text{H}_2\text{C}=\text{O}$.

^e These bands were observed in the experiments on generation of SiH_2 by photolysis of $\text{H}_2\text{Si}(\text{N}_3)_2$ in CO-containing Ar matrices after short-term annealing of the matrices. The difference of these frequencies from those recorded in the experimental studies of the interaction $\text{Si} + \text{H}_2\text{C}=\text{O}$ is probably due to the matrix effect owing to different experimental conditions.⁵¹ The band at 2054 cm⁻¹ observed in the experiments on photolysis of SiH_4 in CO-containing Ar matrices and assigned to SiH_xCO associates⁵³ could correspond to $\text{H}_2\text{Si} \cdot \text{CO}$ complex.

^f Unambiguous assignment of these bands to the vibrational modes listed below is impossible.

^g Arithmetic mean of the frequencies of the maxima of two overlapping bands.

and large, complexation with dinitrogen has little effect on the natural vibrational frequencies of CAs. However, it can strongly affect their electronic absorption spectra (EAS). It is complexation that seems to be responsible for unusually large frequency shift of the bands in the EAS of silylenes SiClMe , SiHMe , and SiMe_2 on going from Ar to N_2 matrices.⁵⁰

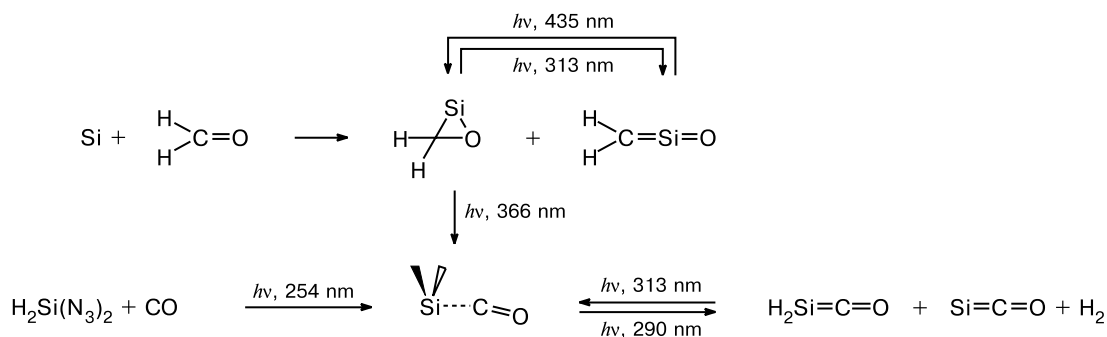
The IR spectra of several complexes of PbHal_2 and SnCl_2 with CO and NO were recorded³⁶ in Ar matrices (their experimental frequencies are listed in Table 4). The $\nu(\text{C—O})$ and $\nu(\text{N—O})$ frequencies of the complexes are higher than those of unbound CO and NO. Based on this fact and by analogy with the complexes formed by salts of transition metals with CO, it was concluded³⁶ that the detected complexes of CAs with CO and NO are σ -complexes containing CAs coordinated to the C and N atoms, respectively. As far as we know, no quantum-chemical calculations of such complexes have been reported so far. Based on the frequency shifts of the stretching vibrations of dihalo-substituted CAs upon complexation with N_2 , CO, and NO (see Tables 1 and 4), one can conclude that the σ -donor properties of the ligands weaken in the order $\text{CO} > \text{NO} > \text{N}_2$.³⁶ Analogously, the $\nu(\text{C—O})$ frequency shifts upon complexation with dihaloplumbylenes (see Table 4) point that the strength of complexes decreases on going from fluorides to iodides,³⁶ because the frequency shift decreases in this order. This fact cannot be due to the increase in the mass of halogen, because the frequency shift of $\nu(\text{C—O})$ upon isotope substitution by ^{13}C is nearly the same for both unbound and bound CO, which points to a small contribution of the displacement coordinates of the CAs fragment in the complex to a given normal vibration and, hence, to the fact that the masses of substituents in the CAs cannot have a pronounced effect on a given frequency. Going from $\text{Cl}_2\text{Sn} \cdot \text{CO}$ and $\text{Cl}_2\text{Sn} \cdot \text{NO}$ to $\text{Cl}_2\text{Pb} \cdot \text{CO}$ and $\text{F}_2\text{Pb} \cdot \text{NO}$ causes an insignificant decrease in the $\nu(\text{C—O})$ and $\nu(\text{N—O})$ frequencies, whereas the relative shift of the $\nu(\text{E—Cl})$ frequencies in the complex of dichloroplumbylene ($\sim 2\%$) is 1.5 times

smaller than in the complex of dichlorostannylene with CO (3%, see Table 4). This can serve as an indication of weakening of the acceptor ability of plumbylenes compared to stannylenes.

The interaction of Si atoms with formaldehyde and SiH_2 (generated by photolysis of diazidosilane) with CO in an Ar matrix (see Scheme 4) resulted in a complex $\text{H}_2\text{Si} \cdot \text{CO}$ ⁵¹ characterized by several vibrational frequencies (see Table 4) and an UV absorption band at 296 nm. The $\nu(\text{C—O})$ frequency of this complex is lower than that of unbound CO. Earlier,⁵² in the reaction of SiMe_2 generated by photolysis of matrix isolated *cyclo*-(Me_2Si)₆ with CO present in matrices also gave a product characterized by a low $\nu(\text{C—O})$ frequency (1962 cm^{-1} , see Table 4) and by an UV band at 342 nm. The last-named band was also observed⁵² in the interaction of SiMe_2 with CO in N_2 and CO matrices and in glassy 3-methylpentane matrices. Semiempirical AM1 and MNDO quantum-chemical calculations as well as HF/3-21G calculations of the system $\text{SiMe}_2 + \text{CO}$ gave contradictory results,⁵² thus precluding unambiguous conclusions about the structure of the product, namely, is this product a $\text{Me}_2\text{Si} \cdot \text{CO}$ complex or a silaketene $\text{Me}_2\text{Si}=\text{C}=\text{O}$.

A detailed B3LYP/6-31G** study⁵¹ of the PES of the system $\text{SiH}_2 + \text{CO}$ (the $\text{SiMe}_2 + \text{CO}$ system was also considered) showed that the $\text{H}_2\text{Si} \cdot \text{CO}$ complex corresponds to a global minimum and the energy of its formation is $26.5\text{ kcal mol}^{-1}$. According to calculations,⁵¹ planar silaketene structure corresponds to a transition state (TS) of inversion in the complex rather than an energy minimum on the PES. Changes in the geometry of reagents upon complexation are as follows: a slight shortening of Si—H bonds (from 1.530 to 1.512 Å), a small elongation of the C—O bond (from 1.138 to 1.148 Å), and some increase in the H—Si—H angle (from 91.2 to 99.2°). The CO molecule is arranged nearly normal to the SiH_2 plane, namely, the angle between the axis of the Si—C bond and the SiH_2 plane is 89.0° while the angle Si—C—O is 167.4°. The Si—C bond is rather short (1.891

Scheme 4



Conditions: Ar matrix, 12 K.

Å). According to calculations,⁵¹ the $\nu(\text{C}=\text{O})$ frequency of the complex decreases, though the magnitude of the decrease strongly depends on the computational method employed, namely, it is 8.7 cm^{-1} (CISD/6-31G**), 52.5 cm^{-1} (QCISD/6-31G**), 75.6 cm^{-1} (MP2/6-31G**), 80.1 cm^{-1} (B3LYP/6-31G**), and 96.2 cm^{-1} (B3LYP/6-311+G**). At the same time, lower-level computational methods (RHF/6-31G** and CISD/V95) predict an increase in the $\nu(\text{C}=\text{O})$ frequency upon complexation.⁵¹ That is why the experimentally observed product of interaction between SiMe_2 and CO was not identified based on predictions of quantum-chemical calculations.⁵² By and large, the frequencies of the $\text{H}_2\text{Si}\cdot\text{CO}$ complex and their shifts relative to the starting reagents obtained in B3LYP/6-31G** and especially B3LYP/6-311+G** calculations⁵¹ are in good agreement with experimental values.⁵¹ The geometric parameters of the $\text{H}_2\text{Si}\cdot\text{CO}$ complex obtained from more recent MP2/6-31G(d) calculations⁵⁷ are close to those found earlier.⁵¹ The G2 calculated⁵⁷ heat of formation of the $\text{H}_2\text{Si}\cdot\text{CO}$ complex at 298 K is $22.0\text{ kcal mol}^{-1}$. Calculations⁵⁷ also showed that complexation proceeds barrierlessly. Kinetic measurements performed in that study⁵⁷ revealed that the rate of the gas-phase reaction between SiH_2 and CO approaches the value determined exclusively by collision frequency.

B3LYP/6-31G** calculations⁵¹ also correctly reproduced the experimentally observed⁵² shift of the $\nu(\text{C}=\text{O})$ frequency of the $\text{Me}_2\text{Si}\cdot\text{CO}$ complex. A greater decrease in this frequency for the complex with SiMe_2 compared to the complex with SiH_2 can be associated⁵¹ with larger contribution of back donation to the coordination bond, which comes from the dimethylsilylene LEP owing to the greater s-character of the LEP. As a consequence, in the $\text{Me}_2\text{Si}\cdot\text{CO}$ complex the angle between the axis of the coordination bond and the SiC_2 plane of the silylene fragment is 107.5° , thus being much larger than in the $\text{H}_2\text{Si}\cdot\text{CO}$ complex, while the coordination bond is somewhat shorter (1.886 Å).⁵¹

Complexes of silylenes SiRR' ($\text{R}, \text{R}' = \text{Mes}, \text{Mes}; \text{Mes}, \text{Bu}^t; \text{Mes}, 2,6\text{-Pr}_i_2\text{C}_6\text{H}_3\text{O}; \text{Me}, \text{Me}$) with CO were also detected using UV spectroscopy in glassy hydrocarbon matrices.⁵⁸ SiMe_2 was generated by photolysis of *cyclo*-(SiMe_2)₆ while the other silylenes were generated by photolysis of the corresponding compounds $\text{RR}'\text{Si}(\text{SiMe}_3)_2$. The absorption band maxima were observed at 354 and 284 nm ($\text{Mes}_2\text{Si}\cdot\text{CO}$), at 338 and 290 nm ($\text{Mes}(\text{Bu}^t)\text{Si}\cdot\text{CO}$), at 328 nm ($\text{Mes}(2,6\text{-Pr}_i_2\text{C}_6\text{H}_3\text{O})\text{Si}\cdot\text{CO}$), and at 345 nm ($\text{Me}_2\text{Si}\cdot\text{CO}$).⁵⁸ The last-mentioned value coincides with the published data⁵² within the limits of experimental error. The observed absorption bands of the complexes lie in the spectral region characteristic of complexes of silylenes with other Lewis bases.⁴ Annealing of matrices resulted in dimeriza-

tion and oligomerization of complexes accompanied by loss of CO.⁵⁸

From the results of the studies of complexes of CAs with CO it follows that the $\nu(\text{C}=\text{O})$ frequency increases when carbon monoxide interacts with dihalo-substituted stannylenes and plumbylenes and decreases when CO reacts with dialkyl-substituted silylenes (see Table 4). The reason for this fact is unclear and requires further investigations.

No systematic matrix isolation studies of the interaction of CAs with H_2 have been carried out so far. However, in some cases it was observed that the bands of silylenes generated by photochemically induced hydrogen elimination from the precursor molecule in matrices were shifted relative to the bands of the same silylenes produced using other methods that exclude the presence of H_2 molecule in the matrix cage containing CA. As can be seen in Scheme 4, the $\text{H}_2\text{Si}\cdot\text{CO}$ complex exposed to light ($\lambda = 290\text{ nm}$) transformed into two products, namely, SiCO characterized by a known⁵⁹ absorption band at 1898.2 cm^{-1} and a product characterized by a band at 1906.3 cm^{-1} (see Ref. 51). Exposure of the latter product to the light with $\lambda = 313\text{ nm}$ again led to the formation of $\text{H}_2\text{Si}\cdot\text{CO}$ complex. Close values of the frequencies of both bands and the photochemical behavior of the newly formed product suggested that photolysis of $\text{H}_2\text{Si}\cdot\text{CO}$ near the maximum of its absorption band causes elimination of the H_2 molecule which can either escape from the matrix cage by expending the kinetic energy stored during the decomposition or remain in the cage, thus inducing the shift of the SiCO band (due to formation of a loosely bound complex). This complex, $\text{H}_2\cdot\text{SiCO}$, again transformed into $\text{H}_2\text{Si}\cdot\text{CO}$ on exposure to light with longer wavelength.⁵¹ Analogously, studies on the mutual photochemical transformations of intermediates of composition $\text{C}_2\text{H}_2\text{Si}$ and H_3NSi revealed the formation of complexes of 1-silacyclopropylylidene⁵⁴ and iminosilylene⁵⁵ with H_2 molecule, respectively (see Table 4). The $\text{HN}=\text{Si}\cdot\text{H}_2$ complex characterized by an UV absorption maximum at 250 nm in Ar matrix transformed into $\text{N}=\text{SiH}\cdot\text{H}_2$ after exposure to UV light with $\lambda = 193\text{ nm}$ and into $\text{H}_2\text{Si}=\text{NH}$ after exposure to light with $\lambda = 254\text{ nm}$. These products again transformed into $\text{HN}=\text{Si}\cdot\text{H}_2$ on irradiation at $\lambda = 254\text{ nm}$ and at $\lambda > 310$ or $\lambda = 222\text{ nm}$, respectively.⁵⁵ Annealing of matrices was accompanied by hydrogen elimination from $\text{HN}=\text{Si}\cdot\text{H}_2$ and by an increase in the band intensities of $\text{Si}=\text{NH}$, which was not transformed into $\text{H}_2\text{Si}=\text{NH}$ on exposure to light with $\lambda = 254\text{ nm}$, but isomerized into $\text{N}=\text{SiH}$ upon photolysis at $\lambda = 193\text{ nm}$.⁵⁵ The H—H vibrational modes of this complex appeared to be IR active (the corresponding band was observed⁵⁵ at 4178 cm^{-1} and then exhibited a characteristic shift to 2994 cm^{-1} in the spectrum of deuterated complex $\text{DN}=\text{Si}\cdot\text{D}_2$, see Table 4).

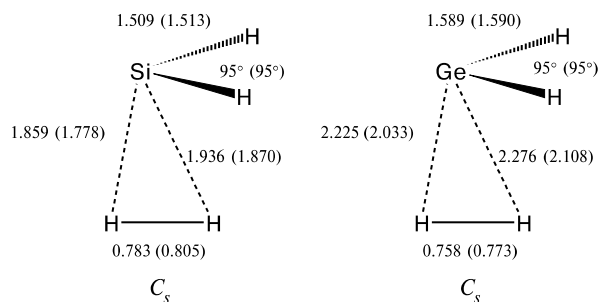


Fig. 2. Structures of complexes $\text{H}_2\text{Si} \cdot \text{H}_2$ and $\text{H}_2\text{Ge} \cdot \text{H}_2$ obtained from QCISD/6-311G(d,p) and B3LYP/6-311++G(3df,2pd) calculations (figures in parentheses).⁶⁰ Given are the bond lengths (in Å) and angles (in degrees).

Geometric parameters of the starting molecules

Molecule	$r(\text{H}-\text{H})/\text{\AA}$	$r(\text{E}-\text{H})/\text{\AA}$	$\omega(\text{H}-\text{E}-\text{H})/\text{deg}$
H_2	0.744 (0.743)	—	—
GeH_2	—	1.592 (1.596)	91.8 (90.9)
SiH_2	—	1.516 (1.523)	92.6 (91.6)

No quantum-chemical calculations of these experimentally detected complexes have been carried out so far. However, prototype complexes $\text{H}_2\text{Si} \cdot \text{H}_2$ ^{60–63} and $\text{H}_2\text{Ge} \cdot \text{H}_2$ ⁶⁰ were calculated; their structures and geometric parameters obtained from QCISD/6-311G(d,p) and B3LYP/6-311++G(3df,2pd) calculations⁶⁰ are shown in Fig. 2. These structures imply some polarization of the H—H bond and, hence, IR activity of the corresponding vibrational mode. Complex $\text{H}_2\text{Si} \cdot \text{H}_2$ readily isomerizes into stable SiH_4 ; the activation barrier calculated for $T = 273$ K with inclusion of ZPE is 5.3 (QCISD(T)/6-311G++(3df,2pd)//QCISD/6-311G(d,p)) and 4.8 (B3LYP/6-311++G(3df,2pd)) kcal mol^{–1}. An analogous isomerization of the $\text{H}_2\text{Ge} \cdot \text{H}_2$ complex requires the overcoming of a higher barrier (both methods gave a value of 14.0 kcal mol^{–1} calculated for $T = 273$ K with inclusion of ZPE).⁶⁰ As a consequence, the reaction of SiH_2 with H_2 was found to be rather fast,^{64,65} whereas kinetic measurements using laser flash photolysis technique revealed no interaction between GeH_2 and H_2 .⁶⁰

Matrix IR spectroscopy studies of the interaction of several silylenes with O_2 were reported.^{56,66–68} It was reliably established that the reaction of SiF_2 with O_2 in argon matrices results in a complex $\text{F}_2\text{Si} \cdot \text{O}_2$ (see Table 4), which undergoes isomerization into difluorosiladioxirane on exposure to light ($\lambda < 365$ nm).⁵⁶ The structure of the complex is unknown. Dichlorosilylene reacted with O_2 only on exposure to light ($\lambda < 575$ nm) to give dichlorosiladioxirane,⁵⁶ whereas the formation of dimethylsiladioxirane from SiMe_2 and O_2 occurred spontaneously.⁶⁸ No complexes of SiCl_2 and SiMe_2 with dioxygen were detected. Apparently, the product of interaction between SiMe_2 and O_2 in low-temperature O_2 matrix, which was identified^{66,67} as a complex, is in fact also a siladioxirane.⁶⁸

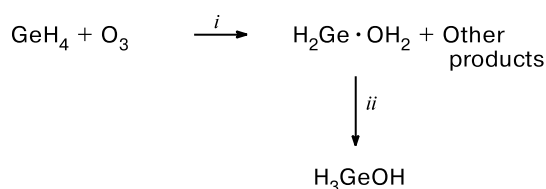
From the results presented in this Section it follows that CAs tend to form complexes with such diatomic molecules as CO , NO , O_2 , and even with so weak Lewis bases as N_2 and H_2 . Complexes with O_2 and H_2 can be formed in the initial stages of reactions with CAs and undergo subsequent transformations into products containing valence bonds only. At the same time the reaction with O_2 can proceed without intermediate complexation. In the case of CO , NO , and N_2 , complexation is the exclusive reaction channel for less reactive (dihalo-substituted) CAs. However, SiH_2 can react with CO under particular conditions to give some other products including those formed involving transformations of the corresponding complex (see Scheme 4), which, however, is the most thermodynamically stable product. At present, it is impossible to reveal any general trends in changes in the acceptor ability of CAs toward these weak bases, because the available experimental data are limited. Nevertheless, for complexes of dihalo-substituted CAs with N_2 it was shown^{34–36} that the strength of complexes increases on going to heavier CAs and as the atomic number of the halogen substituent decreases. One of the most surprising results obtained in the studies mentioned above is different directions of shifts of the $\nu(\text{C}-\text{O})$ band upon complexation of CO with dihalo-substituted CAs and silylenes SiR_2 ($\text{R} = \text{H}, \text{Me}$). This has no reliable explanation as yet.

Complexes of carbene analogs with H_2O

Water simultaneously possesses the properties of a rather strong Lewis base (due to the central O atom) and a rather strong H-acid. Additionally, the H_2O molecule is a highly reactive species. Nevertheless, a number of complexes of silylenes and germylenes with H_2O , in which the CAs act as the Lewis acids, were detected using matrix IR spectroscopy.

A donor-acceptor complex $\text{H}_2\text{Ge} \cdot \text{OH}_2$ was obtained by exposing a mixture of GeH_4 with ozone in Ar matrix at 14–18 K to light ($\lambda > 380$ nm).⁶⁹ Photolysis by harder radiation led to isomerization of the complex into an insertion product, H_3GeOH (Scheme 5).

Scheme 5



Conditions: Ar matrix, 14–18 K; *i.* $\lambda > 380$ nm; *ii.* λ 290–1000 nm.

Table 5. Vibrational frequencies (ν) of $\text{H}_2\text{Ge}\cdot\text{OH}_2$ complex and its isotopomers⁶⁹

GeH ₂ fragment			H ₂ O fragment						Assignment	
ν/cm ⁻¹			ν/cm ⁻¹							
GeH ₂	GeHD*	GeD ₂	H ₂ ¹⁶ O	H ₂ ¹⁸ O	HD ¹⁶ O	HD ¹⁸ O	D ₂ ¹⁶ O	D ₂ ¹⁸ O		
1813.6	1811.6									ν ^s (O—H/D)
1777.2	1782.0									δ(H/D—O—H/D)
	1307.4	1308.9								ν ^{as} (O—H/D)
	1287.0	1281.6								
1794.4										2δ(HGeH)
897.8										δ(HGeH)
		1293.3								2δ(DGeD)
		646.4								δ(DGeD)

* The $\delta(\text{DGeH})$ band is hidden by the bands of the starting differently deuterated molecules $\text{GeH}_x\text{D}_{4-x}$.

Table 6. Vibrational frequencies (ν/cm^{-1}) of complexes $\text{H}(\text{HO})\text{Si}\cdot\text{OH}_2$ and $\text{H}(\text{HO})\text{Ge}\cdot\text{OH}_2$.⁷³

E	$\nu(\text{E}-\text{H})$	$\nu(\text{E}-\text{O})^*$
Si	1929.4	778.5
Ge	1763.1	609.1

* Stretching vibration frequencies of the Si—O and Ge—O valence bonds.

The observed vibrational frequencies⁶⁹ of complex $\text{H}_2\text{Ge}\cdot\text{OH}_2$ and its isotopomers are listed in Table 5. Since the isotopic substitution in each fragment of the complex of GeH_2 with H_2O affects only the frequencies of this fragment, they are listed in Table 5 separately. Complexation causes some weakening of the Ge—H and O—H bonds, as is indicated by a decrease in the $\nu(\text{Ge}-\text{H})$ and $\nu(\text{O}-\text{H})$ frequencies relative to the corresponding frequencies of matrix isolated GeH_2 (1887 and 1864 cm^{-1})⁷⁰ and H_2O (3736 and 3639.4 cm^{-1}).⁷¹ Both H/D and $^{16}\text{O}/^{18}\text{O}$ isotopic substitutions permitted the assignment of vibrational bands of the complex and made it possible to conclude that two H atoms bound to the Ge atom in the complex are nonequivalent. Later on, this was confirmed by the results of DFT and *ab initio* calculations.⁷² According to MP2/TZP(2df,2pd) and B3LYP/TZP(2df,2pd) calculations (hereafter, MP2 and B3LYP calculations, respectively), the fragments GeH_2 and H_2O lie in two non-parallel planes (the MP2 and B3LYP calculated angle between these planes is 28.7 and 27.9°, respectively), being rotated by $\sim 90^\circ$ about the axis of the Ge—O bond. The MP2 (B3LYP) calculated dihedral angles determined by the O—H and Ge—H bonds relative to the Ge—O bond are 175.4 (170.5) and 82.6 (78.7) for one O—H bond and 62.0 (56.4) and -30.8 (-35.4)° for the other O—H bond. The Ge—O separation is 2.214 (MP2) and 2.268 Å (B3LYP) while the distance

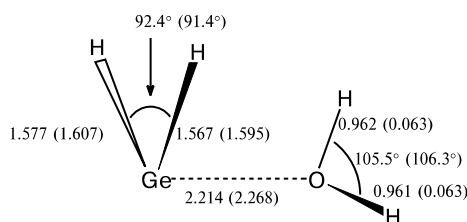
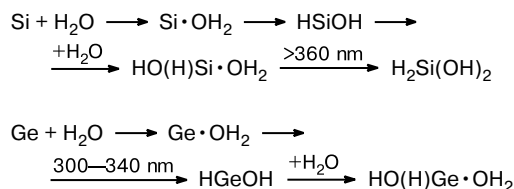


Fig. 3. Structure of a complex of GeH_2 with H_2O calculated by the MP2/TZP(2df,2pd) and B3LYP/TZP(2df,2pd) (figures in parentheses) methods.⁷² Given are the bond lengths (in Å) and angles (in degrees).

from the O atom to the GeH_2 plane is 2.202 (MP2) and 2.255 Å (B3LYP) (Fig. 3).

The geometric parameters of the GeH_2 and H_2O fragments of the complex differ only slightly from the corresponding parameters of the starting molecules, GeH_2 and H_2O . The complexation energy calculated⁷² at different levels of theory (including MP4//MP2 and CCSD//MP2) is ~ 9 kcal mol^{-1} . Not only the Ge—H bond but also the O—H bonds in the complex are nonequivalent; however, nonequivalence of the O—H bonds has a much weaker effect on their stretching vibration frequencies. According to calculations of complexes containing the HOD fragment, nonequivalence of the O—H(D) bonds causes a doublet splitting of the $\nu(\text{O}-\text{H})$ and $\nu(\text{O}-\text{D})$ frequencies, the frequency difference for each doublet being only 3–4 cm^{-1} . Resolution of the doublet components in the experiment is difficult. An analogous splitting of the Ge—H and Ge—D vibrational frequencies in the complexes containing a GeHD fragment exceeds 30 cm^{-1} . By and large, the calculated frequencies⁷² are in good agreement with the experimental data.⁶⁹

Complexes $\text{H}(\text{OH})\text{Si}\cdot\text{OH}_2$ and $\text{H}(\text{OH})\text{Ge}\cdot\text{OH}_2$ were detected using IR spectroscopy in the course of reactions of Si and Ge atoms with H_2O in Ar matrices in the presence of a large excess of water.⁷³



Conditions: Ar matrix, 15 K.

The reaction of Si atoms proceeded spontaneously but accelerated upon exposure of the matrix to light with $\lambda > 360 \text{ nm}$. Germanium atoms reacted only as the matrix was exposed to light with wavelengths lying between 300 and 340 nm. A decrease in the concentration of water in the matrix was accompanied by the formation of corresponding CAs, that is, HSiOH and HGeOH. Prolonged photolysis caused transformation of the $\text{H(OH)Si} \cdot \text{OH}_2$ complex into $\text{H}_2\text{Si(OH)}_2$, a product of silylene insertion into the O—H bond of the H_2O fragment. The experimental frequencies of the complexes are listed in Table 6. The bands of the H_2O fragment in the complexes were not recorded because their intensities were too low to be detected against the background of broad intense bands of unbound excess water. A feature of these complexes is an increase in the E—H vibrational frequencies and a decrease in the E—O vibrational frequencies (for HSiOH, Fermi-resonance of $\nu(\text{Si—H})$ with the first overtone of $\delta(\text{HSiO})$ gives two frequencies, 1885.2 and 1849.1 cm^{-1} , $\nu(\text{Si—O}) = 850.5 \text{ cm}^{-1}$; for HGeOH, $\nu(\text{Ge—H}) = 1741.3 \text{ cm}^{-1}$ while $\nu(\text{Ge—O}) = 661.3 \text{ cm}^{-1}$).⁷³

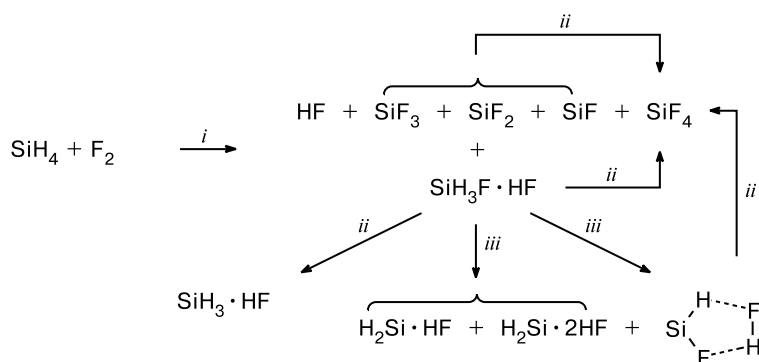
Complexes of carbene analogs with HHal and RHal

Carbene analogs can be involved in insertion reactions into E—Hal (E = C, Si, Ge, Sn, H) bonds.^{1,4,5} Because the Hal atom has a LEP, organic halo derivatives can act as Lewis bases, whereas halogen hydrides can also act as both bases and H-acids.

Matrix IR spectroscopy studies of the interaction of SiH_4 , GeH_4 , and their deuterated analogs with F_2 were reported.⁷⁴ The formation of complexes of EH_2 and EHF (E = Si, Ge) with HF was detected. The most important transformations observed in the interaction of SiH_4 with F_2 are shown in Scheme 6. The reactions of SiD_4 , GeH_4 , and GeD_4 with F_2 obeyed the same pattern, but SiD_4 was less reactive during the deposition of the matrix, while germanes gave two different complexes of GeHF with HF. The reaction products were identified based on investigation of their photochemical transformations, analysis of spectral information, and results of HF/DZP quantum-chemical calculations.⁷⁴ The frequencies of the detected complexes of silylenes and germynes with HF are listed in Table 7.

According to quantum-chemical calculations,⁷⁴ the reaction of SiH_2 with HF can produce three types of complexes. These are a planar complex $\text{HSiH} \cdot \text{HF}$ ($\Delta E = -1.6 \text{ kcal mol}^{-1}$) characterized by coordination of the H atom of the fragment HF to a silylene hydrogen, a planar complex $\text{H}_2\text{Si} \cdot \text{HF}$ ($\Delta E = -3.9 \text{ kcal mol}^{-1}$) in which silylene acts as a base and forms a hydrogen bond, and a complex $\text{H}_2\text{Si} \cdot \text{FH}$ ($\Delta E = -4.8 \text{ kcal mol}^{-1}$) where silylene acts as a Lewis acid and the F atom is coordinated to the Si atom. The calculated energies of these complexes are very close to one another; this precludes unambiguous conclusions which of them are observed in the experiments. Experiments⁷⁴ revealed the formation of two types of complexes of SiH_2 with HF. Based on analysis of the frequencies and results quantum-chemical calculations and on the studies of the mechanisms of the processes in question, it was concluded that in both experimentally detected complexes the SiH_2 fragment is coordinated to HF in the same way but in one complex the HF molecule is additionally coordinated to the second HF molecule (see Table 7). The character of coordination of SiH_2 to HF in these complexes was not established.

Scheme 6



Conditions: Ar matrix, 13 K; *i.* Deposition, photolysis >290 and $>220 \text{ nm}$; *ii.* annealing, 25—30 K; *iii.* photolysis $\lambda >290$ and $\lambda >220 \text{ nm}$.

Table 7. Vibrational frequencies (ν) of the complexes of CAs EH_2 and EHF ($\text{E} = \text{Si}, \text{Ge}$) with HF ⁷⁴ and the corresponding frequencies of EH_2 , EHF ¹² and HF ⁷⁴ (figures in parentheses) recorded in Ar matrices

Complex	ν/cm^{-1}				Assignment	Complex	ν/cm^{-1}				Assignment
	SiH_2	SiD_2	GeH_2	GeD_2			HSiF	DSiF	HGeF	DGeF	
$\text{H}_2\text{E} \cdot 2\text{HF}$	3828.1 (3954)	2798 (2876.6)	3730.6 (3954)	2739 (2876.6)	$\nu(\text{H/D}-\text{F})$ $\nu(\text{H/D}-\text{F})^b$	<i>cyclo-</i>	3796 ^a	2784 ^a	3662.1	2693.2	$\nu(\text{H/D}-\text{F})$
	1985.7 (1973.3)	1448.3 (1439.1)	1870.7 (1839)	1346.8 (1338)	$\nu^{\text{as}}(\text{E}-\text{H/D})$ $\nu^{\text{as}}(\text{E}-\text{H/D})^d$	$\text{FEH} \cdot \text{HF}$	1908.0 (1913.1)	1385.4 (1387.4)	1784.6	1287.8	$\nu(\text{E}-\text{H/D})$ $\nu(\text{E}-\text{H/D})^c$
$\text{H}_2\text{E} \cdot \text{HF}$	1942.8	1424.7	1819.0	1312.5	$\nu^{\text{as}}(\text{E}-\text{H/D})$		865.5 (859.0)	—	—	—	$\delta(\text{H/D}-\text{E}-\text{H/D})$ $\delta(\text{H/D}-\text{E}-\text{H/D})^c$
							751.6 (833.7)	—	—	—	$\nu(\text{E}-\text{F})$ $\nu(\text{E}-\text{F})^c$
						$\text{HGeF} \cdot \text{HF}$	—	—	3717.2 1795.2	2732.1 1296.2	$\nu(\text{H/D}-\text{F})$ $\nu(\text{E}-\text{H/D})$

^a Tentative assignment.^b In HF .^c In HEF .^d In EH_2 .

According to calculations, SiHF and HF also form several types of complexes with close-lying energies. Among them, the most stable are a cyclic complex with simultaneous coordination of HF to the H and F atoms of silylene ($\Delta E = -5.2 \text{ kcal mol}^{-1}$, see Scheme 6) and a complex $\text{HSiF} \cdot \text{HF}$ with a $0.34 \text{ kcal mol}^{-1}$ higher energy, in which the F atom of fluorosilylene forms a hydrogen bond with the HF fragment. Calculations failed to find a structure corresponding to the complex containing silylene acting as a Lewis base. Based on the calculated stability order, the experimentally detected complex of SiHF with HF was identified as a cyclic species. A related complex of GeHF with HF was also assigned a cyclic structure, while the second complex of GeHF with HF was assigned the structure $\text{HGeF} \cdot \text{HF}$.⁷⁴

Thus, none of the detected⁷⁴ complexes of CAs with HF was identified as a complex in which the CA acts as a Lewis acid owing to the acidic properties of the central atom.

UV spectroscopy studies^{21,22} of germynes generated in glassy hydrocarbon matrices containing *cyclo*- $\text{C}_6\text{H}_{11}\text{Cl}$ and PhCl revealed a number of new bands that were blue shifted by 5–110 nm relative to the bands of unbound germynes and assigned to their complexes with these organochlorine compounds.^{21,22} Annealing of matrices containing complexes led to loss of the complexes but gave no stable products of the interaction of germynes with the $\text{C}-\text{Cl}$ bonds of *cyclo*- $\text{C}_6\text{H}_{11}\text{Cl}$ and PhCl . A complex of GeMe_2 with allyl chloride was obtained in a similar way. Annealing of hydrocarbon matrices containing this complex also led to loss of the complex and to the formation of $\text{Me}_2\text{Ge}(\text{All})\text{Cl}$, a product of germylene insertion into the $\text{C}-\text{Cl}$ bond.^{21,22} Coordination of germylene to the Cl atom rather than the double bond of allyl chloride (see the next Section) was supported by the

fact that no formation of complexes of GeMe_2 with olefins was observed under these experimental conditions.²¹ Complexes $\text{Me}_2\text{Si} \cdot \text{Br}_3\text{CH}$ ²⁷ and $\text{Me}_2\text{Si} \cdot \text{Cl}_4\text{C}$ ²⁸ were detected using liquid-phase laser flash photolysis, positions of their UV absorption bands and the extinction coefficients were determined, and the kinetics of loss was studied.

Matrix IR spectroscopy studies⁷⁵ revealed the formation of a complex $\text{F}_2\text{Sn} \cdot \text{ClMe}$ in the low-temperature Ar matrix upon co-deposition of SnF_2 and MeCl in a mixture with excess Ar. The complex was characterized by two vibrational bands of $\nu(\text{Sn}-\text{F})$ (Table 8). No bands of the MeCl fragment in the complex were recorded because of much lower intensities (see below). Annealing of matrices led to disappearance of the complex and to the formation of an oligomerization product $(\text{SnF}_2)_x$. No product of difluorostannylene insertion into the $\text{C}-\text{Cl}$ bond was observed in the matrix.

The PES of the system $\text{F}_2\text{Sn} + \text{MeCl}$ was studied by the *ab initio* $\text{HF}/3-21\text{G}(\text{d})$, semiempirical PM3 ,⁷⁵ and (in this work) by $\text{PBE}/\text{TZ2P}$ ⁷⁶ methods. PBE calculations were carried out using the PRIRODA program.⁷⁷ Full geometry optimization and vibrational frequency calculations were performed using the triple-zeta type basis sets: $(5\text{s}2\text{p}) [3\text{s}2\text{p}]$ for H , $(11\text{s}6\text{p}2\text{d}) [6\text{s}3\text{p}2\text{d}]$ for C and F , $(15\text{s}11\text{p}2\text{d}) [10\text{s}6\text{p}2\text{d}]$ for Cl , and $(21\text{s}17\text{p}12\text{d}) [15\text{s}12\text{p}8\text{d}]$ for Sn (the primitive Gaussian basis sets are given in parentheses, while the contracted basis sets are given in brackets). The PRIRODA program employs the electron density expansion over an auxiliary uncontracted basis set:⁷⁸ $(5\text{s}2\text{p})$ for H , $(10\text{s}3\text{p}3\text{d}1\text{f})$ for C and F , $(14\text{s}3\text{p}3\text{d}1\text{f}1\text{g})$ for Cl , and $(23\text{s}3\text{p}3\text{d}1\text{f}1\text{g})$ for Sn . The characters of the stationary points located were determined by calculating the eigenvalues of the matrix of the second derivatives of energy. The thermodynamic functions were calculated

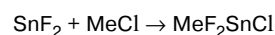
Table 8. Experimental and PBE/TZ2P calculated vibrational frequencies (ν) of complexes of SnF_2 with organic compounds and the corresponding frequencies of the starting reagents in Ar matrices

Compound	$\nu^{\text{as}}(\text{Sn}-\text{F})$	$\nu^{\text{s}}(\text{Sn}-\text{F})$	$\rho(\text{C}-\text{H})$	$\nu(\text{C}\equiv\text{C})$	$\nu(\equiv\text{C}-\text{H})$	Method	Reference
F_2Sn	571	593	—	—	—	Experiment	75
	554	568				PBE	This work
$\text{F}_2\text{Sn}\cdot\text{ClMe}$	543	567	—	—	—	Experiment	75
	521	539				PBE	This work
$\text{F}_2\text{Sn}\cdot\text{ClPh}$	549	566	753, 764	—	—	Experiment	79
PhCl	—	—	743	—	—	Experiment	79
$\text{F}_2\text{Sn}\cdot\text{PhH}$	542	564	688, 696	—	—	Experiment	79
	525	542	671			PBE, structure 1	This work
	525	542	691			PBE, structure 2	This work
PhH	—	—	677	—	—	Experiment	79
			656			PBE	This work
$\text{F}_2\text{Sn}\cdot 2\text{PhH}$	538	562	—	—	—	Experiment	79
$\text{F}_2\text{Sn}\cdot\text{PhMe}$	536	563	740	—	—	Experiment	79
PhMe	—	—	731	—	—	Experiment	79
$\text{F}_2\text{Sn}\cdot\text{C}_2\text{H}_4$	537.5	551.5	—	—	—	Experiment	80
	528	542				PBE	This work
$\text{F}_2\text{Sn}\cdot\text{Hp}^a$	540	565	—	2088	3256	Experiment	81, 82
	530	532		2086	3370	PBE	This work
Hp	—	—	—	2127	3318	Experiment	81, 82
$\text{Si}^{35}\text{Cl}_2$	501.3	512.2	—	—	—	Experiment	83
	483	490				PBE	This work
$^{35}\text{Cl}_2\text{Si}\cdot\text{C}_2\text{H}_2$	482.4	^b	792	1965	3294, 3271	Experiment	83
	455	467				PBE	This work
C_2H_2	—	—	737	—	3302, 3289	Experiment	83
			738		3352	PBE	This work
$^{35}\text{Cl}_2\text{Si}\cdot\text{C}_2\text{HD}$	482.2	^b	709	^b	3328, 2576	Experiment	83
C_2HD	—	—	683	1856	3341, 2587	Experiment	83
$^{35}\text{Cl}_2\text{Si}\cdot\text{C}_2\text{D}_2$	482	^b	583	1747	2433	Experiment	83
C_2D_2	—	—	543	—	2442	Experiment	83

^a Hp stands for hept-1-yne.^b The band is hidden by the bands of the starting reagents.

using the harmonic oscillator—rigid rotator model. The PBE calculated energies of the structures involved in complexation of SnF_2 with organic substrates and in the subsequent reactions are listed in Table 9. A local minimum corresponding to the complex $\text{F}_2\text{Sn}\cdot\text{ClMe}$ was located; the structure of the complex is shown in Fig. 4. The geometry of the complex is strongly affected by the dipole-dipole interaction between the starting molecules, namely, the vectors of the dipole moments of SnF_2 and MeCl are oppositely directed and the dipole moment of the complex (0.3 D) is approximately equal to the difference of dipole moments of SnF_2 and MeCl (2.4, and 2.2 D (HF), respectively). The complexation energy is 8.4 (PBE) and 10.8 kcal mol⁻¹ (MP2//HF).⁷⁵ According to HF calculations,⁷⁵ only two vibrational frequencies of the complex are markedly shifted relative to the corresponding frequencies of MeCl and SnF_2 and at the same time have rather high intensities. These vibrations are described by superpositions $\nu^{\text{as}}(\text{SnF}_2) + \delta^{\text{as}}(\text{C}-\text{H})$ and $\nu^{\text{s}}(\text{SnF}_2) + \nu(\text{C}-\text{Cl})$; their frequencies (694 and 721 cm⁻¹) are close

to the calculated frequencies of free SnF_2 (730 and 748 cm⁻¹, respectively). Other band intensities are by nearly an order of magnitude lower, thus providing an explanation for the absence of the $\nu(\text{C}-\text{Cl})$ band in the recorded IR spectra. According to calculations, an insertion reaction



is energetically favorable ($\Delta E = -27.3$ (PBE) and -47.4 kcal mol⁻¹ (HF)) but has a high activation barrier (47.0 kcal mol⁻¹ (MP2//HF calculations⁷⁵)), which precludes the formation of insertion product under low-temperature matrix conditions.

Complexes of carbene analogs with aromatic and unsaturated compounds

Aromatic compounds can act as weak bases. There are experimental and theoretical data that point to the exist-

Table 9. Total energies ($E/\text{a.u.}$) of and total energy differences ($\Delta E/\text{kcal mol}^{-1}$) between participants of complexation reactions of SnF_2 with organic substrates and subsequent cycloaddition (insertion) obtained from PBE calculations

Structure	$-E$	$-E_0^b$	$\Delta E + \text{ZPE}$
SnF_2	6224.6009	6224.5979	
ClMe	499.9017	499.8649	
$\text{F}_2\text{Sn} \cdot \text{ClMe}^c$	6724.5173	6724.4763	-8.4
$\text{CH}_3\text{SnF}_2\text{Cl}^d$	6724.5470	6724.5064	-27.3
PhH	232.0211	231.9236	
$\text{F}_2\text{Sn} \cdot \text{PhH}^e$ (1)	6456.6333	6456.5316	-6.4
$\text{F}_2\text{Sn} \cdot \text{PhH}^e$ (2)	6456.6331	6456.5314	-6.2
C_2H_4	78.5022	78.4527	
$\text{F}_2\text{Sn} \cdot \text{C}_2\text{H}_4^e$	6303.1137	6303.0597	-5.7
<i>cyclo</i> - $\text{SnF}_2\text{CH}_2\text{CH}_2^f$	6303.0507	6302.9970	33.6
C_2H_2	77.2519	77.2258	
$\text{F}_2\text{Sn} \cdot \text{C}_2\text{H}_2^e$	6301.8625	6301.8324	-5.4
<i>cyclo</i> - $\text{SnF}_2\text{CHCH}^f$	6301.8149	6301.7830	25.6
Hp^g	273.6194	273.4543	
$\text{F}_2\text{Sn} \cdot \text{Hp}^e$	6498.2388	6498.0699	-11.1
<i>cyclo</i> - $\text{SnF}_2\text{CHCC}_5\text{H}_{11}^f$	6498.1831	6498.0131	24.5

^a Calculated for $T = 0$ K.

^b $E_0 = E + \text{ZPE}$.

^c σ -Complex.

^d Insertion product.

^e π -Complex.

^f Cycloaddition product.

^g Hept-1-yne.

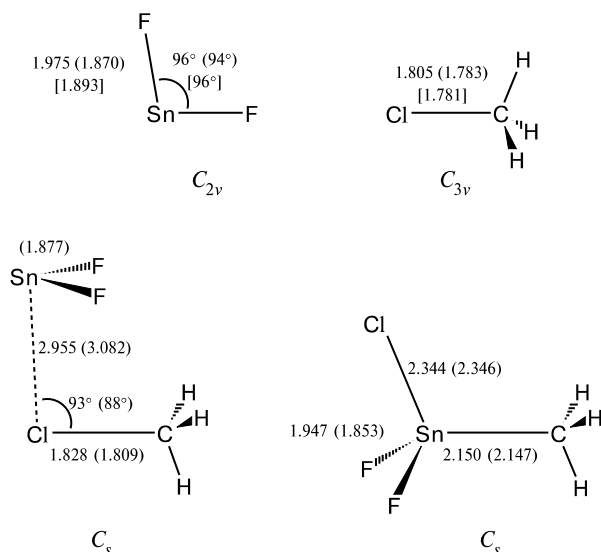


Fig. 4. Selected geometric parameters (bond lengths in Å, angles in degrees) of the SnF_2 and MeCl molecules, the $\text{F}_2\text{Sn} \cdot \text{MeCl}$ complex, and of the addition product obtained from PBE/TZ2P and HF/3-21G(d) calculations (figures in parentheses⁷⁵) and the experimental data for SnF_2 ⁴⁰ and MeCl ⁸⁴ (figures in brackets). Shown are the symmetry groups.

ence of carbene complexes with aromatics.⁸⁵ The results of studies on the effect of the nature of precursor on the

position of the UV absorption band maximum of GeMe_2 generated in glassy hydrocarbon matrices suggested the formation of complexes with aromatic compounds.⁸⁶ Stable crystalline complexes of Sn^{II} salts with aromatics were described⁸⁷ (in the crystalline phase, compounds of divalent tin have, as a rule, an ionic structure and cannot therefore be considered as CAs, *i.e.*, a kind of species in which the carbene center forms covalent bonds with substituents⁸⁸).

We carried out a thorough matrix IR spectroscopy study⁷⁹ of complexes of SnF_2 with benzene, toluene, and chlorobenzene. The complexes were characterized by the bands of out-of-plane deformation vibrations $\rho(\text{C}-\text{H})$ of the aromatic fragment and by the $\nu(\text{Sn}-\text{F})$ stretching vibrations (see Table 8). The appearance of shifted $\rho(\text{C}-\text{H})$ bands in the IR spectrum complex points that the SnF_2 fragment approaching the aromatic ring is out of the ring plane. The IR spectra of the PhCl and PhH fragments in the complexes exhibit two $\rho(\text{C}-\text{H})$ bands. Since this vibration is not symmetry degenerated, the appearance of two new frequencies indicates the formation of two complexes differing in orientation of F atoms relative to the C—H bonds and having identical stabilities. Earlier,⁸⁹ splitting of the $\rho(\text{C}-\text{H})$ band of benzene was observed in the formation of its complex with H_2O . This was explained by the presence of several minima on the PES of the benzene—water system, which have close-lying energies and correspond to different orientations of the O—H bond relative to the aromatic ring. The IR spectrum of complex $\text{F}_2\text{Sn} \cdot \text{PhMe}$ exhibits only one shifted $\rho(\text{C}-\text{H})$ frequency. Probably, the formation of the second complex is prevented by the Me group.

In the case of interaction between SnF_2 and PhCl one would also expect coordination of difluorostannylene to the Cl atom and, as a consequence, the appearance of a $\nu(\text{C}-\text{Cl})$ band and a second set of $\nu(\text{Sn}-\text{F})$ bands of this complex in the IR spectrum. However, the $\nu(\text{Sn}-\text{F})$ bands of the complex could match those of the complex of SnF_2 coordinated to the π -system (*cf.* the $\nu(\text{Sn}-\text{F})$ frequencies of $\text{F}_2\text{Sn} \cdot \text{PhH}$ and $\text{F}_2\text{Sn} \cdot \text{ClMe}$ in Table 8), while the $\nu(\text{C}-\text{Cl})$ vibration could be of low intensity similarly to the case for complex $\text{F}_2\text{Sn} \cdot \text{ClMe}$. Thus, the formation of complex $\text{F}_2\text{Sn} \cdot \text{ClPh}$ cannot be ruled out, though it was not detected in the experiment. We can also suggest that this complex is more loosely bound than the complex in which SnF_2 is coordinated to the π -system of PhCl .

Complex $\text{F}_2\text{Sn} \cdot (\text{PhH})_2$ (see Table 8) was detected after the benzene concentration in the matrix increased from 1 to 2%.⁷⁹ Here, the ability of stannylene to form coordination bonds involving its vacant p-orbital is fully utilized. This complex is characterized by somewhat larger $\nu(\text{Sn}-\text{F})$ frequency shifts compared to the $\text{F}_2\text{Sn} \cdot \text{PhH}$ complex (see Table 8). Observation of the $\rho(\text{C}-\text{H})$ bands of this complex was precluded by extremely high intensity of the corresponding band of unbound benzene.

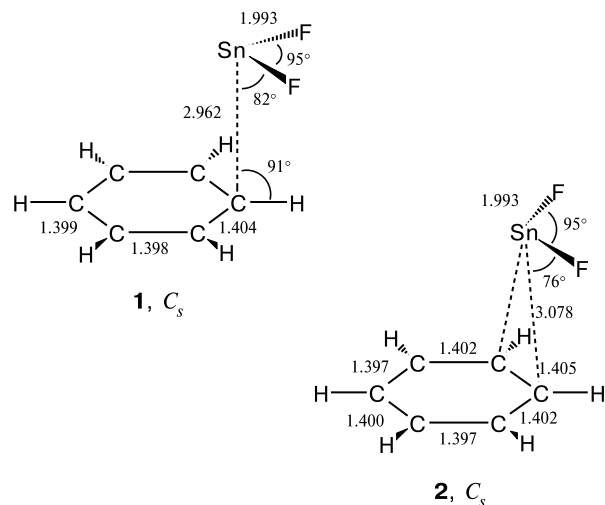


Fig. 5. Structures of complexes of SnF_2 with benzene obtained from PBE/TZ2P calculations (bond lengths are given in Å and angles are given in degrees). Shown are the symmetry groups of the structures.

The $\nu(\text{Sn}-\text{F})$ frequency shift upon complexation with the aromatic compounds under study somewhat increases in the order PhCl , PhH , PhMe (see Table 8). This implies the same order of strengthening of the complexes and is consistent with the expected order of increasing the strength of the complexes due to the changes in the electronic effects of substituents in the aromatic ring.

To obtain more detailed information on the interaction of SnF_2 with benzene, we carried out PBE/TZ2P calculations of the complexes. The structures obtained are shown in Fig. 5 while the frequencies and energies are listed in Tables 8 and 9, respectively. Calculations of the system $\text{SnF}_2\text{---PhH}$ predict the existence of two structurally similar π -complexes **1** and **2** (see Fig. 5). In both complexes the plane of the SnF_2 molecule is nearly parallel to the benzene ring plane. In structure **1**, the Sn atom is coordinated to a C atom while in structure **2** it is coordinated to two C atoms, being located above the midpoint of C—C bond. Both complexes belong to the same symmetry group and have identical sets of IR active modes. Noteworthy is that the energies of both complexes differ only slightly ($\Delta E = -6.4$ and -6.2 kcal mol $^{-1}$); therefore, the concentrations of both species in the matrix must also be nearly equal. According to calculations, complexes **1** and **2** are characterized by the same $\nu(\text{Sn}-\text{F})$ frequencies and different $\rho(\text{C}-\text{H})$ frequencies (671 and 691 cm $^{-1}$, see Table 8). As mentioned above, it is this spectral pattern that was observed in the matrix IR spectrum.⁷⁸

The first matrix IR spectroscopy study⁷⁹ of the complex of this CA with benzene gave two vibrational frequencies (564 and 551 cm $^{-1}$). The $\nu^{\text{as}}(\text{Sn}-\text{F})$ frequency of the complex $\text{F}_2\text{Sn}\cdot\text{PhH}$ (542 cm $^{-1}$) observed in our experimental study⁷⁹ differs from the previous⁸⁰ value (551 cm $^{-1}$). Besides, no $\rho(\text{C}-\text{H})$ frequencies of the aro-

matic fragment of the complex $\text{F}_2\text{Sn}\cdot\text{PhH}$ were detected earlier.⁸⁰ Unfortunately, we cannot analyze the reasons for these discrepancies because no detailed description of the experiments⁸⁰ was reported.

A complex of SnF_2 with ethylene was detected⁸⁰ by matrix IR spectroscopy and characterized by two $\nu(\text{Sn}-\text{F})$ frequencies (see Table 8). No shifted ethylene bands in the complex were observed, probably, because of low band intensities due to the high symmetry of the ethylene molecule. Based on qualitative considerations, it was concluded that the SnF_2 molecule is coordinated to the π -bond of ethylene molecule. Observation of this complex provided an explanation for the necessity of using Sn^{II} salts as co-catalysts of several industrially important processes of olefin transformations.⁸⁰

In preparing this review we carried out PBE/TZ2P calculations of a complex of SnF_2 with ethylene and of the corresponding cycloaddition product, 1,1-difluorostannocyclopropane (1,1-difluorostannirane). The structures obtained are shown in Fig. 6 and their frequencies and energies are listed in Tables 8 and 9, respectively. According to calculations, the geometric parameters of SnF_2 and ethylene in the π -complex differ insignificantly from the corresponding values for free molecules. The C=C bond in the complex (1.344 Å) is slightly longer than in the unbound ethylene (1.334 Å); the same holds for the Sn—F bonds (1.992 and 1.975 Å, respectively). The plane of the SnF_2 molecule in the π -complex is nearly parallel to the plane in which the ethylene molecule lies. The complex of SnF_2 with ethylene is less stable than the complex with benzene ($\Delta E = -5.7$ kcal mol $^{-1}$). The calculated $\nu(\text{Sn}-\text{F})$ frequency shifts in the complex with ethylene (26 and 25 cm $^{-1}$) are close to the corresponding characteristics of $\text{F}_2\text{Sn}\cdot\text{PhH}$ (28 and 26 cm $^{-1}$). The formation of 1,1-difluorostannocyclopropane is energetically unfavorable ($\Delta E = 33.6$ kcal mol $^{-1}$). Earlier,⁹⁰ an MP2 study of the reactions of SiF_2 , GeF_2 , and SnF_2 with ethylene suggested the formation of π -complexes with energies $\Delta E = -3.9$, -3.4 , and -4.8 kcal mol $^{-1}$, respectively. The enthalpies (ΔH) of cycloaddition reactions of SiF_2 , GeF_2 ,

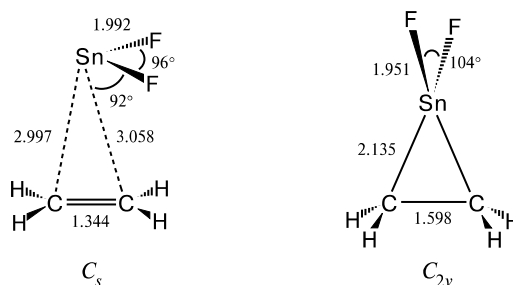


Fig. 6. Structures of a complex of SnF_2 with ethylene and of the cycloaddition product of SnF_2 to C_2H_4 obtained from PBE/TZ2P calculations (bond lengths are given in Å and angles are given in degrees). Shown are the symmetry groups of the structures.

and SnF_2 were -22.8 , 19.9 and $35.1 \text{ kcal mol}^{-1}$, respectively. These energy characteristics are in good agreement with the results of the PBE calculations carried out in this work. Unfortunately, no vibrational frequencies necessary for the interpretation of the IR spectra of complexes were reported.⁹⁰

A related complex of SnF_2 with asymmetrical hept-1-yne was stabilized in a low-temperature Ar matrix and characterized^{81,82} by the $\nu(\text{Sn}-\text{F})$, $\nu(\text{C}\equiv\text{C})$, and $\nu(\text{C}-\text{H})$ IR bands (see Table 8). The presence of two last-mentioned bands in the spectrum unambiguously indicates that SnF_2 is coordinated to the triple bond of the hept-1-yne molecule. The existence of a π -complex in the system $\text{SnF}_2 + \text{hept-1-yne}$ was predicted^{81,82} by semiempirical AM1 and PM3 methods. To obtain a more detailed and reliable picture of the interaction of SnF_2 with various organic molecules, in this work we performed PBE/TZ2P calculations of the complexes and cycloaddition products of SnF_2 to acetylene and hept-1-yne. The calculated structures are presented in Fig. 7 and the characteristic frequencies and energies are listed in Tables 8 and 9, respectively. According to calculations, both complexes are structurally similar. The plane of the SnF_2 molecule in these π -complexes is nearly parallel to the plane in which the $\text{C}\equiv\text{C}$ bond lies. The geometric parameters of the SnF_2 and alkyne fragments in the π -complexes differ insignificantly from the corresponding values for free molecules. For instance, the $\text{C}\equiv\text{C}$ bond lengths in the complexes (1.211 and 1.218 \AA) are slightly longer than in the acety-

lene and hept-1-yne molecules (1.207 and 1.212 \AA , respectively). The $\text{Sn}-\text{F}$ bonds are also elongated from 1.975 \AA in difluorostannylene to 1.989 and 1.998 \AA in the complexes with acetylene and hept-1-yne, respectively. Complexation of difluorostannylene with acetylene affects the geometry of the SnF_2 fragment to a much lesser extent than complexation with hept-1-yne in spite of similarity of both structures. This is consistent with the order of interaction energies for both complexes ($\Delta E = -5.4$ and $-11.1 \text{ kcal mol}^{-1}$, respectively, see Table 9).

The reaction of SnF_2 with mono-substituted alkynes can lead to two types of π -complexes differing in the orientation of $\text{Sn}-\text{F}$ bonds relative to the substituent in the alkyne fragment. According to semiempirical calculations,^{81,82} the orientation shown in Fig. 7 is more stable. This effect was explained^{81,82} by the interaction between the SnF_2 and hept-1-yne dipoles. A similar picture also follows from the results of our PBE calculations.

The calculated frequency shifts of SnF_2 in the complexes with acetylene (23 and 20 cm^{-1}) are smaller than in the complex with hept-1-yne (24 and 36 cm^{-1}), which can be reasonably explained by different complexation energies. The set of frequencies for which calculations predict a rather large shift upon π -complexation is consistent with the shifted frequencies observed experimentally. According to calculations, cycloaddition of SnF_2 to acetylene and hept-1-yne is energetically unfavorable ($\Delta E = 25.6$ and $24.5 \text{ kcal mol}^{-1}$, respectively). The results of *ab initio* calculations of the PES of the reaction of SnF_2 with acetylene⁹¹ also indicate that this process is highly endothermic (the thermal effect is $16.5 \text{ kcal mol}^{-1}$). That is why the interaction of SnF_2 with alkynes under matrix conditions stops at the π -complexation stage.

All experimentally observed π -complexes of SnF_2 with unsaturated organic compounds as well as the σ -com-

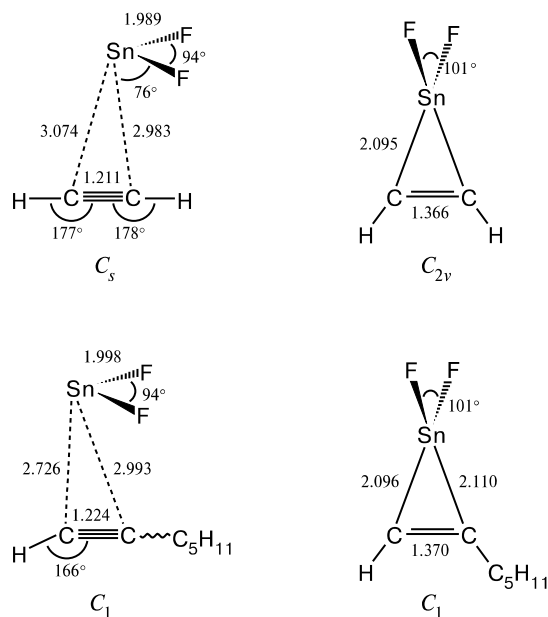


Fig. 7. Main geometric parameters of π -complexes of SnF_2 with acetylene and hept-1-yne and of the corresponding cycloaddition products obtained from PBE/TZ2P calculations (bond lengths are given in Å and angles are given in degrees). Shown are the symmetry groups of the structures.

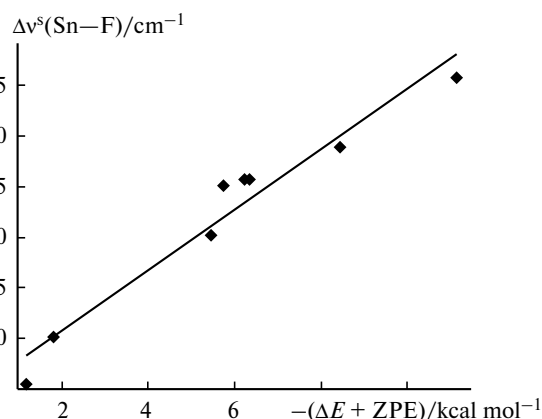
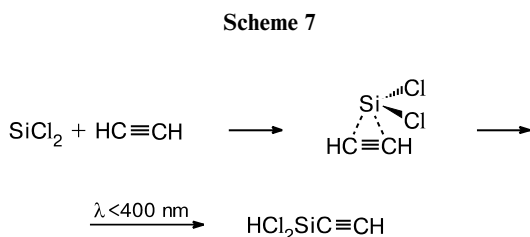


Fig. 8. Correlation between the PBE/TZ2P calculated complexation energies of SnF_2 with Lewis bases and the frequency shifts of the $\text{Sn}-\text{F}$ symmetric vibration of these complexes; $y = 3.0x + 4.8$, $R^2 = 0.95$. Obtained using the data listed in Tables 2, 8, and 9.

plexes with MeCl and N₂ were characterized by the $\nu(\text{Sn}-\text{F})$ frequencies (see Tables 1 and 8). A common mechanism of electronic interaction in these complexes manifests itself in a good correlation (Fig. 8, $R^2 = 0.95$) between the complexation energies $-(\Delta E + \text{ZPE})$ and the PBE/TZ2P calculated frequency shifts of the Sn—F symmetric vibration (see Tables 2, 8 and 9). It should be emphasized that this correlation was plotted using the data for both σ -complexes and π -complexes. Thus, the frequency shift of the symmetric vibration $\Delta\nu^s$ can serve as a criterion for the strength of complexes of different ligands with the same CAs.

Recently, we have studied the interaction of SiCl₂ with acetylene.⁸³ Co-condensation of SiCl₂ generated by pyrolysis of Si₂Cl₆ with C₂H₂, C₂DH, and C₂D₂ in Ar matrices produced complexes with these isotopomers. Similarly to the complex of SnF₂ with hept-1-yne, they were characterized not only by the Si—Cl stretching vibration frequencies but also by the frequencies of the acetylene fragment (see Table 8). The shifts of the vibrational frequencies of the complex and of unbound acetylene upon H/D-substitution are close, which substantiates correctness of the tentative band assignment and indicates minor changes in the geometry and force field in the complex compared to the starting reagents. Photolysis of complexes with UV light ($\lambda < 400$ nm) caused isomerization of the complexes into the product of silylene insertion into C—H bond (Scheme 7).



Based on the efficiency of photolysis of the complex at different wavelengths, the position of absorption maximum was estimated at about 300 nm. This seems to be somewhat lower than the reported position of absorption maximum of SiCl₂ isolated in Ar matrix (315 nm).⁹² In this connection it should be noted that the shift of the absorption band of the S₀—S₁ electronic transition toward shorter wavelengths upon the formation of complexes with Lewis bases is a characteristic feature of CAs.^{4,12}

Conclusion

The available experimental data and the results of calculations unambiguously indicate that complexation with weak Lewis bases is typical of CAs and plays an important role in chemistry of these reactive intermediates. The ther-

modynamic stability of donor-acceptor complexes and the activation barriers to their rearrangements into stable reaction products vary over a wide range depending on the nature of CAs and substrate. Joint studies involving matrix IR spectroscopy and modern quantum-chemical methods provide an efficient tool of investigations of complexes of CAs.

The authors express their gratitude to D. N. Laikov for kindly providing a version of his PRIRODA program.

This work was financially supported by the Russian Foundation for Basic Research (Project Nos. 03-03-32564 and 04-03-32838), Russian Academy of Sciences (Program "Theoretical and Experimental Investigations on the Nature of Chemical Bonding and Mechanisms of the Most Important Chemical Reactions and Processes" of the Chemistry and Materials Science Division and Program "Thermal Physics and Mechanics of Intense Energy Action" of the Presidium of the Russian Academy of Sciences), Ministry of Science and Education of the Russian Federation (Federal Target Research and Technological Program "Research and Development on Priority Avenues of Science and Technology"), and the Russian Federation Presidential Program for support of leading research schools (Grant NSh-1987.2003.3).

References

1. O. M. Nefedov, A. I. Ioffe, and L. G. Menchikov, *Khimiya karbenov* [Chemistry of Carbenes], Moscow, Khimiya, 1990, 304 pp. (in Russian)
2. O. M. Nefedov, M. P. Egorov, A. I. Ioffe, L. G. Menchikov, P. S. Zuev, V. I. Minkin, B. Ya. Simkin, and M. N. Glukhovtsev, *Pure Appl. Chem.*, 1992, **64**, 265.
3. S. P. Kolesnikov, *Zh. Vses. Khim. O-va im. D. I. Mendeleeva*, 1979, **24**, 505 [*Mendeleev Chem. J.*, 1979, **24** (Engl. Transl.)].
4. P. P. Gaspar and R. West, in *The Chemistry of Organic Silicon Compounds*, Eds Z. Rappoport and Y. Apeloig, Wiley, Chichester, 1998, Vol. 1, p. 2463.
5. W. P. Neumann, *Chem. Rev.*, 1991, **91**, 311.
6. M. P. Egorov and P. P. Gaspar, in *Encyclopedia of Inorganic Chemistry*, Ed. R. B. King, Wiley, New York, 1995, Vol. 3, 1229.
7. E. G. Rochow, *Silicon and Silicones*, Springer-Verlag, Berlin, 1987.
8. T. Motooka and J. E. Greene, *J. Appl. Phys.*, 1986, **59**, 2015.
9. A. Sekiguchi, T. Tanaka, M. Ichinohe, K. Akiyama, and S. Tero-Kubota, *J. Am. Chem. Soc.*, 2003, **125**, 4962.
10. P. P. Gaspar, M. C. Xiao, D. H. Pae, D. J. Berger, T. Haile, T. Q. Chen, D. Q. Lei, W. R. Winchester, and P. Jiang, *J. Organomet. Chem.*, 2002, **646**, 68.
11. S. N. Tandura, C. N. Gurkova, and A. I. Gusev, *Zh. Strukt. Khim.*, 1990, **31**, 154 [*J. Struct. Chem. (USSR)*, 1990, **31** (Engl. Transl.)].
12. S. E. Bogdanov, M. P. Egorov, V. I. Faustov, and O. M. Nefedov, in *The Chemistry of Organic Germanium, Tin and*

- Lead Compounds*, Ed. Z. Rappoport, Wiley, 2002, Vol. 2, Part 1, 749.
13. R. Becerra and R. Walsh, in *Research in Chemical Kinetics*, Eds R. G. Compton and G. Hancock, Elsevier, Amsterdam, 1995, **3**, p. 263.
 14. S. P. Kolesnikov, B. L. Perl'mutter, and O. M. Nefedov, *Izv. Akad. Nauk SSSR. Ser. Khim.*, 1979, 37 [*Bull. Acad. Sci. USSR, Div. Chem. Sci.*, 1979, **28** (Engl. Transl.)].
 15. J. Barrau and G. Rima, *Coord. Chem. Rev.*, 1998, **178–180**, 593.
 16. P. D. Lickiss, in *The Chemistry of Tin*, Ed. P. G. Harrison, Blackie, London, 1989, 221.
 17. A. Márquez and J. F. Sanz, *J. Am. Chem. Soc.*, 1992, **114**, 10019.
 18. T. Ohtaki, Y. Kabe, and W. Ando, *Organometallics*, 1993, **12**, 4.
 19. W. Ando, K. Hagiwara, and A. Sekiguchi, *Organometallics*, 1987, **6**, 2270.
 20. G. R. Gilette, G. H. Noren, and R. West, *Organometallics*, 1989, **8**, 487.
 21. W. Ando, H. Itoh, and T. Tsumuraya, *Organometallics*, 1989, **8**, 2759.
 22. W. Ando, H. Itoh, T. Tsumuraya, and H. Yoshida, *Organometallics*, 1988, **7**, 1880.
 23. G. Levin, P. K. Das, C. Bilgren, and C. L. Lee, *Organometallics*, 1989, **8**, 1206.
 24. S. P. Kolesnikov, M. P. Egorov, A. S. Dvornikov, V. A. Kuz'min, and O. M. Nefedov, *Izv. Akad. Nauk SSSR. Ser. Khim.*, 1988, 2654 [*Bull. Acad. Sci. USSR, Div. Chem. Sci.*, 1988, **37** (Engl. Transl.)].
 25. M. P. Egorov, A. S. Dvornikov, M. B. Ezhova, V. A. Kuz'min, S. P. Kolesnikov, and O. M. Nefedov, *Metalloorgan. Khim.*, 1991, **4**, 1178 [*Organomet. Chem. USSR*, 1991, **4** (Engl. Transl.)].
 26. M. P. Egorov and O. M. Nefedov, *Metalloorgan. Khim.*, 1992, **5**, 106 [*Organomet. Chem. USSR*, 1992, **5** (Engl. Transl.)].
 27. M. B. Taraban, V. F. Plyusnin, O. S. Volkova, V. P. Grivin, T. V. Leshina, V. Ya. Lee, V. I. Faustov, M. P. Egorov, and O. M. Nefedov, *J. Phys. Chem.*, 1995, **99**, 14719.
 28. M. B. Taraban, O. S. Volkova, V. F. Plyusnin, A. O. Kruppa, T. V. Leshina, M. P. Egorov, and O. M. Nefedov, *J. Phys. Chem., A*, 2003, **107**, 4096.
 29. S. Cradock and A. J. Hinchcliffe, *Matrix Isolation*, Cambridge University Press, Cambridge, 1975.
 30. V. A. Korolev and O. M. Nefedov, *Adv. Phys. Org. Chem.*, 1995, **30**, 1.
 31. M. E. Jacox, *Chem. Soc. Rev.*, 2002, **31**, 108.
 32. M. Hidai and Y. Mizobe, *Chem. Rev.*, 1995, **95**, 1115.
 33. J. Ho, R. J. Drake, and D. W. Stephan, *J. Am. Chem. Soc.*, 1993, **115**, 3792.
 34. A. V. Lalov, S. E. Boganov, V. I. Faustov, M. P. Egorov, and O. M. Nefedov, *Izv. Akad. Nauk. Ser. Khim.*, 2003, 504 [*Russ. Chem. Bull., Int. Ed.*, 2003, **52**, 526].
 35. S. E. Boganov, V. I. Faustov, M. P. Egorov, and O. M. Nefedov, *Izv. Akad. Nauk. Ser. Khim.*, 1998, 1087 [*Russ. Chem. Bull.*, 1998, **47**, 1054 (Engl. Transl.)].
 36. D. Tevault and K. Nakamoto, *Inorg. Chem.*, 1976, **15**, 1282.
 37. K. P. Huber and G. Herzberg, *Constants of Diatomic Molecules*, Van Nostrand Reinhold, New York, 1979.
 38. M. Fujitake and E. Hirota, *Spectrochim. Acta, A*, 1994, **50**, 1345.
 39. M. J. Tsuchiya, H. Honjou, K. Tanaka, and T. Tanaka, *J. Mol. Struct.*, 1995, **352–353**, 407.
 40. I. Hargittai and O. M. Nefedov, *J. Mol. Struct.*, 1982, **82**, 107.
 41. K. V. Ermakov, B. S. Butayev, and V. P. Spiridonov, *J. Mol. Struct.*, 1991, **248**, 143.
 42. M. Tacke, Ch. Klein, D. J. Stufkens, A. Oskam, P. Jutzi, and E. A. Bunte, *Z. anorg. allg. Chem.*, 1993, **619**, 865.
 43. D. F. Shriver, *Acc. Chem. Res.*, 1970, **3**, 231.
 44. W. W. Schoeller and R. Schneider, *Chem. Ber. Recl.*, 1997, **130**, 1013.
 45. G. Maass, R. H. Hauge, and J. L. Margrave, *Z. anorg. allg. Chem.*, 1972, **392**, 295.
 46. H. Huber, E. P. Kundig, G. A. Ozin, and A. V. Voet, *Can. J. Chem.*, 1974, **52**, 95.
 47. G. A. Ozin and A. V. Voet, *J. Chem. Phys.*, 1972, **56**, 4768.
 48. J. W. Hastie, R. H. Hauge, and J. L. Margrave, *High Temp. Sci.*, 1971, **3**, 56.
 49. H. P. Reisenauer, G. Mihm, and G. Maier, *Angew. Chem.*, 1982, **94**, 864.
 50. G. Maier, G. Mihm, H. P. Reisenauer, and D. Littmann, *Chem. Ber.*, 1984, **117**, 2369.
 51. G. Maier, H.-P. Reisenauer, and H. Egenolf, *Organometallics*, 1999, **18**, 2155.
 52. C. A. Arrington, J. T. Petty, S. E. Payne, and W. C. K. Haskins, *J. Am. Chem. Soc.*, 1988, **110**, 6240.
 53. D. Milligan and M. E. Jacox, *J. Chem. Phys.*, 1970, **52**, 2594.
 54. G. Maier, H. Pacl, H. P. Reisenauer, A. Meudt, and R. Janoschek, *J. Am. Chem. Soc.*, 1995, **117**, 12712.
 55. G. Maier and J. Glatthaar, *Angew. Chem., Int. Ed. Engl.*, 1994, **33**, 473.
 56. A. Patyk, W. Sander, J. Gauss, and D. Cremer, *Chem. Ber.*, 1990, **123**, 89.
 57. R. Becerra, J. P. Cannady, and R. Walsh, *J. Phys. Chem., A*, 2001, **105**, 1897.
 58. M.-A. Pearsall and R. West, *J. Am. Chem. Soc.*, 1988, **110**, 7228.
 59. R. R. Lembke, R. F. Ferrante, and W. Weltner, *J. Am. Chem. Soc.*, 1977, **99**, 416.
 60. R. Becerra, S. E. Boganov, M. P. Egorov, V. I. Faustov, O. M. Nefedov, and R. Walsh, *Can. J. Chem.*, 2000, **78**, 1428.
 61. C. Sosa and H. B. Schlegel, *J. Am. Chem. Soc.*, 1984, **106**, 5847.
 62. A. Sax and G. Olbrich, *J. Am. Chem. Soc.*, 1985, **107**, 4868.
 63. M. S. Gordon, D. R. Gano, J. S. Binkley, and M. J. Frisch, *J. Am. Chem. Soc.*, 1986, **108**, 2191.
 64. J. M. Jasinsky, *J. Phys. Chem.*, 1986, **90**, 555.
 65. J. M. Jasinsky, R. Becerra, and R. Walsh, *Chem. Rev.*, 1995, **95**, 1203.
 66. T. Akasaka, S. Nagase, A. Yabe, and W. Ando, *J. Am. Chem. Soc.*, 1988, **110**, 6270.
 67. T. Akasaka, A. Yabe, S. Nagase, and W. Ando, *Nippon Kagaku Kaishi*, 1989, 1440.
 68. A. Patyk, W. Sander, J. Gauss, and D. Cremer, *Angew. Chem., Int. Ed. Engl.*, 1989, **28**, 898.
 69. R. Withnall and L. Andrews, *J. Phys. Chem.*, 1990, **94**, 2351.
 70. G. R. Smith and W. A. Guillory, *J. Chem. Phys.*, 1972, **56**, 1423.

71. G. P. Ayers and A. D. E. Pullin, *Spectrochim. Acta, A*, 1976, **32**, 1629.
72. A. Nowek and J. Leszczynski, *J. Phys. Chem., A*, 1997, **101**, 3784.
73. J. W. Kauffman, R. H. Hauge, and J. L. Margrave, *ACS, Symp. Ser.*, 1982, **179**, 355.
74. T. C. McInnis and L. Andrews, *J. Phys. Chem.*, 1992, **96**, 5276.
75. S. E. Boganov, V. I. Faustov, S. G. Rudyak, M. P. Egorov, and O. M. Nefedov, *Izv. Akad. Nauk. Ser. Khim.*, 1996, 1121 [*Russ. Chem. Bull.*, 1996, **45**, 1061 (Engl. Transl.)].
76. J. P. Perdew, K. Burke, and M. Ernzerhof, *Phys. Rev. Lett.*, 1996, **77**, 3865.
77. D. N. Laikov, Ph.D. (Phys.-Math.) Thesis, Moscow State University, Moscow, 2000 (in Russian).
78. D. N. Laikov, *Chem. Phys. Lett.*, 1997, **281**, 151.
79. S. E. Boganov, M. P. Egorov, and O. M. Nefedov, *Izv. Akad. Nauk. Ser. Khim.*, 1999, 97 [*Russ. Chem. Bull.*, 1999, 1999, **48**, 98 (Engl. Transl.)].
80. P. F. Meier, D. L. Perry, R. H. Hauge, and J. L. Margrave, *Inorg. Chem.*, 1979, **18**, 2051.
81. S. E. Boganov, V. I. Faustov, M. P. Egorov, and O. M. Nefedov, *Izv. Akad. Nauk. Ser. Khim.*, 1994, 54 [*Russ. Chem. Bull.*, 1994, **43**, 47 (Engl. Transl.)].
82. S. E. Boganov, V. I. Faustov, M. P. Egorov, and O. M. Nefedov, *High Temperature and Materials Science*, 1995, **33**, 107.
83. S. E. Boganov, A. V. Lalov, V. I. Faustov, M. P. Egorov, and O. M. Nefedov, *Abstr. VIIth Conf. on the Chemistry of Carbenes and Related Intermediates* (Kazan, Russia, June 23–26, 2003), p. 59.
84. J. J. P. Stewart, *J. Comput. Chem.*, 1991, **12**, 320.
85. R. A. Moss, S. Yan, and K. Krogh-Jespersen, *J. Am. Chem. Soc.*, 1998, **120**, 1088.
86. K. Mochida, S. Tokura, and S. Murata, *J. Chem. Soc., Chem. Commun.*, 1992, 250.
87. D. Y. Gin, M. S. R. Cader, J. R. Sams, and F. Abuke, *Can. J. Chem.*, 1990, **68**, 350 and references cited therein.
88. O. M. Nefedov and M. N. Manakow, *Angew. Chem.*, 1966, **78**, 1966.
89. A. Engdahl and B. Nelander, *J. Phys. Chem.*, 1985, **89**, 2860.
90. S. Sakai, *Int. J. Quantum Chem.*, 1998, **70**, 29.
91. J. A. Boatz, M. S. Gordon, and L. R. Sita, *J. Phys. Chem.*, 1990, **94**, 5488.
92. D. E. Milligan and M. E. Jacox, *J. Chem. Phys.*, 1968, **49**, 1938.

Received March 29, 2004